Evolutionary Ecology Research, 2017, **18**: 123–167

Macroevolutionary patterns in cranial and lower jaw shape of ceratopsian dinosaurs (Dinosauria, Ornithischia): phylogeny, morphological integration, and evolutionary rates

Leonardo Maiorino[1,2], Andrew A. Farke[3], Tassos Kotsakis[1,2] and Paolo Piras[4,5]

[1]*Dipartimento di Scienze, Roma Tre University, Rome, Italy,* [2]*Center for Evolutionary Ecology, Rome, Italy,* [3]*Raymond M. Alf Museum of Paleontology, Claremont, California, USA,* [4]*Dipartimento di Ingegneria Strutturale e Geotecnica, Sapienza Università di Roma, Rome, Italy and* [5]*Dipartimento di Scienze Cardiovascolari, Respiratorie, Nefrologiche, Anestesiologiche e Geriatriche, Sapienza Università di Roma, Rome, Italy*

ABSTRACT

Organisms: Ceratopsians were herbivorous, beaked dinosaurs, ranging from 1 m to 9 m in body length, usually four-footed, and with a bony frill that extended backwards from the cranium over the nape of the neck. Known from Asia, Europe, and North America, they appeared in the Late Jurassic and persisted until the end of the Late Cretaceous.

Questions: Which evolutionary processes drive the phenotypic evolution of skulls and lower jaws within Ceratopsia? What is the degree of morphological integration between the skull and lower jaw, and between the snout and frill among clades? Finally, are there any morphological evolution rate shifts across the ceratopsian phylogeny?

Data: Photographs from 121 ceratopsian skulls and 122 lower jaws in lateral view, both from original photos and published pictures. Fifty-five ceratopsian species are represented in the sample.

Methods: We investigated cranial and lower jaw shape changes across ceratopsians applying two-dimensional geometric morphometrics. We also investigated the morphological variation of the snout and the frill. Using phylogenetic generalized least squares regression, we estimated the degree of phylogenetic signal in size and shape data, as well as in the shape–size relationship. We performed phenotypic evolutionary rate analysis on shape data to describe phenotypic shifts across the phylogeny. Using a rarefied version of Escoufier's RV coefficient, we tested morphological integration between skulls and lower jaws, and between snouts and frills. Finally, we explored the potential link between cranial and frill shape evolution in ceratopsians and the radiation of angiosperms using a linear regression model.

Results: Skull, snout, and frill shapes differ among clades (with the exception of lepto-ceratopsids and protoceratopsids). Lower jaws show distinct morphologies among groups. Size and shape changes are phylogenetically structured. The frill drives the morphological variation

Correspondence: L. Maiorino, Department of Sciences and Center for Evolutionary Ecology, Roma Tre University, Largo S. Leonardo Murialdo 1, 00146 Rome, Italy. email: leonardo.maiorino@uniroma3.it

of the skull, co-varying much more with the lower jaw than with the snout. The frill appears to evolve to co-vary better with the lower jaw in the more morphologically derived clades than in basal ones. A significant linear relationship does exist between cranial shape and angiosperm occurrences, suggesting the hypothesis that the frill evolved in response to changes in dietary compositions associated with the turnover between gymnosperms and angiosperms during the Cretaceous. Significant negative shifts in evolutionary rates characterize skull, snout, frill, and lower jaw shapes, corresponding to nodes where psittacosaurids diverge from other taxa. In contrast, a significant positive shift in skull and snout shape rate of evolution characterizes the clade Ceratopsoidea.

Conclusion: The frill is the main driving force in the overall cranial shape within Ceratopsia and evolved secondarily to better co-vary with the lower jaw to produce a more efficient masticatory apparatus. The changes in frill shape are correlated with the angiosperm diversification that occurred in the Cretaceous and thus correlated with changes in diet. Ceratopsians exhibit a slowdown in the phenotypic evolutionary rate in the Early Cretaceous and an acceleration of the phenotypic rate in the Late Cretaceous.

Keywords: Ceratopsia, evolutionary rates, geometric morphometrics, lower jaw, morphological integration, skull, angiosperms.

INTRODUCTION

Understanding the evolution of phenotypic variation and the phylogenetic history of shape changes has been a primary goal in evolutionary biology since Darwin (Mayr, 1970; Klingenberg and Gidaszewski, 2010; Piras *et al.*, 2011). Geometric morphometrics (GM) is a suitable technique to explore morphological disparity in biological objects. Over the past 20 years, GM has been used to investigate how evolutionary processes drive phenotypic variation among species through time and to evaluate better the phylogenetic relationships among related clades, allometry, and mechanical performance in specific phylogenetic contexts (Rohlf *et al.*, 1996; Monteiro, 2000; Chinnery, 2004a; Mitteroecker *et al.*, 2005; Meloro *et al.*, 2008; Marcolini *et al.*, 2009; Adams and Nistri, 2010; Young *et al.*, 2010; Baab *et al.*, 2012; Bookstein, 2013; Piras *et al.*, 2013). However, GM historically has received comparatively limited attention in the world of dinosaur research. Recently, an increasing number of scientific contributions used this technique to investigate osteological shape variation in dinosaurs (Chapman, 1990; Dodson, 1993; Chinnery, 2004a; Brusatte *et al.*, 2010, 2011; Campione and Evans, 2011; Foth and Rauhut, 2013; Hedrick and Dodson, 2013; Maiorino *et al.*, 2013a, 2013b, 2015a, 2015b). Here, we apply GM to examine anatomical evolution, morphological integration, and potential ecological interactions with plants in the ceratopsians.

The ceratopsians (Dinosauria, Ornithischia, Marginocephalia) represent a well-documented group of herbivorous dinosaurs that were widespread in Laurasia. They apparantly had one of the highest rates of speciation among non-avian dinosaurs (Dodson *et al.*, 2004). Their known evolutionary history spans almost 100 million years, from the early Upper Jurassic [Oxfordian (Xu *et al.*, 2006)] until the end of the Mesozoic (Maastrichtian stage), when non-avian dinosaurs became extinct (Dodson, 1996; Dodson *et al.*, 2004). In the Late Jurassic and Early Cretaceous, ceratopsians were represented by small, morphologically basal taxa and mostly by psittacosaurids. After the late Early Cretaceous this clade experienced a rapid radiation in Asia and, even more so, in North America. During this latter part of their history, the clade experienced both an increase in the number of species and in the variation of cranial ornamentations, including bizarre frill morphologies and the development of nasal and supraorbital horns, typical of North American ceratopsids, or

the 'true' horned dinosaurs of the Late Cretaceous (Chinnery, 2004a; Dodson *et al.*, 2004; Sampson and Loewen, 2010). Thus, within a time span of 50–60 million years, ceratopsians diversified from small (<2 m body length) bipedal and occasionally quadrupedal forms, to huge (>9 m body length) quadrupedal species (Sereno, 1990; Dodson, 1993, 1996; Chinnery, 2004a; Dodson *et al.*, 2004).

Ceratopsia includes four major clades: Psittacosauridae, Protoceratopsidae, Leptoceratopsidae, and Ceratopsidae (the latter includes Centrosaurinae and Chasmosaurinae), and several basal and derived taxa that are not part of distinct radiations [with the exception of a basal clade, Chaoyangsauridae, which includes *Chaoyangsaurus youngi* and *Xuanhuaceratops niei*, from the Late Jurassic of China (Zhao, 1983; Zhao *et al.*, 1999, 2006), and the *Yinlong* + *Hualianceratops* group from the Late Jurassic of China as well (Han *et al.*, 2015)].

The oldest known ceratopsians are *Yinlong downsi* and *Hualianceratops wucaiwanensis*, from the Oxfordian (Late Jurassic) of China. Both ceratopsians were small bipedal dinosaurs (Xu *et al.*, 2006; Han *et al.*, 2015). The 'parrot-beaked' psittacosaurids constitute another basal clade, restricted to central Asia (Siberia, China, Mongolia, and possibly Thailand) during the Early Cretaceous, characterized by a short skull, laterally pronounced jugal horn, short and deep snout, and a scarcely developed frill (Sereno, 1990, 2010; You and Dodson, 2004; Sereno *et al.*, 2010). Psittacosauridae includes at most two genera (*Psittacosaurus* and *Hongshanosaurus*) and at least 10 valid species (You and Dodson, 2004; Sereno, 2010; Sereno *et al.*, 2010).

Leptoceratopsidae includes quadrupedal taxa with total body lengths ranging from 2 to 4 m. They are morphologically distinct from other clades in having a robust jaw bearing highly specialized large teeth, no horns, and a short frill (Makovicky, 2002; Xu *et al.*, 2010a). This clade was widespread in central Asia (Uzbekistan and China) and, more so, in North America during the Late Cretaceous (Makovicky, 2002; You and Dodson, 2004; Ryan *et al.*, 2012a).

Protoceratopsids diversified during the Late Cretaceous in China and Mongolia (Lambert *et al.*, 2001; You and Dodson, 2004; Handa *et al.*, 2012). They were herbivorous quadrupedal dinosaurs characterized by a moderately caudo-dorsally developed frill, short and deep snout, prominent jugals, and a nasal horn (Brown and Schlaikjer, 1940; Maryańska and Osmólska, 1975; Dodson, 1976, 1996; Lambert *et al.*, 2001; You and Dodson, 2004; Handa *et al.*, 2012).

The clade Ceratopsidae comprises herbivorous, quadrupedal, large-bodied (5–8 m body length) dinosaurs (Dodson *et al.*, 2004) and it includes two morphologically distinct sub-clades, Chasmosaurinae and Centrosaurinae. Chasmosaurines possess an elongated and low facial region, long supraorbital horns, nasal horn, reduced frontals, and a well caudo-dorsally expanded frill bearing a triangular squamosal. In contrast, centrosaurines possess a short and deep facial region, a prominent nasal process of the nasal bone, short or absent supraorbital horns (in more derived taxa), enlarged frontals, and a caudo-dorsally expanded frill bearing a squared squamosal (Lehman, 1990; Maidment and Barrett, 2011). The most derived centrosaurines (e.g. *Pachyrhinosaurus*, *Achelousaurus*) had a skull roof characterized by the presence of bosses in place of horns (Fiorillo and Tykoski, 2012; Sampson *et al.*, 2013). Their geographic range was almost entirely restricted to North America, particularly to the portion called Laramidia, formed when increasing global sea levels subdivided the North American continent into two distinct palaeolandmasses: Appalachia in the east and Laramidia in the west (Sampson and Loewen, 2010; Sampson *et al.*, 2010, 2013). Only one exception is known to this biogeographical pattern, the occurrence of the centrosaurine *Sinoceratops zhuchengensis* from the Latest Cretaceous of eastern China (Xu *et al.*, 2010b).

The elongation of the frill seems to be strongly correlated with the elongation of the coronoid process, the lowering of the joint in the lower jaw, and the consequent backwards tilt of the muscle action line (Ostrom, 1966; Mallon and Anderson, 2015). The caudo-dorsal and lateral

expansion of the parieto-squamosal complex produced a consequent elongation and enlargement of the adductor muscles to improve the feeding apparatus in ceratopsids (Ostrom, 1966; Dodson, 1993; Dodson *et al.*, 2004). The frill appears to have evolved primarily as a framework for the jaw muscle attachments (in basal and derived neoceratopsians), and secondarily as a display structure within Ceratopsidae (Makovicky and Norell, 2006). In addition, sexual selection or species recognition may have driven the morphological variation of the ornamentations and not the frill itself. Indeed, the mechanical response may have driven the shape changes of the frill through time. A contentious debate has recently arisen in the literature about the evolution of the 'exaggerated' cranial structures of non-avian dinosaurs (Knell and Sampson, 2011; Padian and Horner, 2011, 2014; Hone *et al.*, 2012; Hone and Naish, 2013; Raia *et al.*, 2015). Whether sexual selection or species recognition was the primary driver of frill evolution remains controversial. In contrast, Raia and colleagues (2015) recently suggested that the evolution of the ornamental complexity of ceratopsian frills is simply a by-product of Cope's rule.

Moreover, distinct cranial morphologies within the two ceratopsid subfamilies probably evolved as an ecological response to a niche partitioning (Henderson, 2010; Mallon and Anderson, 2013, 2014). Henderson (2010) argued that the taller skulls of centrosaurines relative to chasmosaurines were a mechanical response to make a more resistant structure, facilitating dietary niche partitioning. Mallon and Anderson (2013) used linear measurements to investigate the relevance of cranial and lower jaw parameters as potential factors for niche partitioning, confirming some differences in rostral shape and cranial depth between the two subfamilies.

Cranial changes were accompanied by several lower jaw modifications. Basal members possessed a slender lower jaw bearing a short predentary, low and slender dentary with a short coronoid process, and caudally elongated angular and surangular. Later ceratopsians elongated their dentary and predentary, developed a long edentulous anterior jaw, reduced the angular and surangular along with a dorsal elongation of the coronoid process, and displayed a progressive backward displacement of the tooth row (Ostrom, 1966; Tanoue *et al.*, 2009). The most derived clade (Ceratopsidae) had double-rooted dental batteries, whereas basal taxa had the primitive condition of single-rooted functional teeth arranged in a single row (Dodson *et al.*, 2004; You and Dodson, 2004; Tanoue *et al.*, 2009, 2010). Triceratopsins (the most derived chasmosaurines) evolved a lower jaw with a larger and more elongated coronoid process, and a longer dentary than other ceratopsids (Maiorino *et al.*, 2015b).

All of these cranial changes were accompanied by a size increase, and postcranial modifications: the development of skeletal robustness along with a progressive elongation of the trunk, and a shortening of the tail and limbs to support more weight (Chinnery, 2004a; Dodson *et al.*, 2004; Lee *et al.*, 2011). A significant modification in the neoceratopsian postcranium is the development of the syncervical, a complete fusion of the first four cervical vertebra traditionally interpreted as evolving to support a large cranial mass (Farlow and Dodson, 1975; Bakker, 1986; Ostrom and Wellnhofer, 1986; Dodson *et al.*, 2004; Campione and Holmes, 2006). By contrast, recent work suggests that the syncervical evolved before the increase of cranial mass (VanBuren *et al.*, 2015).

Most of the ceratopsian dinosaurs lived in the Cretaceous period, a 'greenhouse' time span characterized by high temperatures (Barron, 1983; Sloan and Barron, 1990; Hay, 2008), elevated carbon dioxide concentrations in the atmosphere (Berner *et al.*, 1983; Arthur *et al.*, 1985; Barron, 1985; Royer *et al.*, 2001), and the ongoing fragmentation of Pangaea. The occurrence of large epicontinental seaways was a significant feature of the Cretaceous (Hancock and Kauffman, 1979; Barron, 1983), such as the Western Interior Seaway (WIS) of North America (Stanley, 2009; Dennis *et al.*,

2013), a shallow sea that flooded the central part of the North American continent and endured for 27 million years [*c*. 95–68 Ma (Sampson and Loewen, 2010; Sampson *et al.*, 2010)]. The continental mass of Laramidia was the consequence of the origin and flooding of the WIS [with the eastern Appalachia continent (Sampson and Loewen, 2010; Sampson *et al.*, 2010, 2013)].

One of the greatest changes in terrestrial ecosystems during the Cretaceous period was the diversification of flowering plants [angiosperms (Barrett and Willis, 2001; Stanley, 2009)], which presumably had a major impact upon dinosaur palaeobiology. Ceratopsians diversified against this global backdrop. Some studies have suggested that there is no link between angiosperm diversity and species diversity in herbivorous dinosaurs (Barrett and Willis, 2001; Barrett and Rayfield, 2006; Butler *et al.*, 2009).

Previous work suggests that ceratopsids ate primarily high-fibrous plants (Ostrom, 1966; Dodson, 1993; Dodson *et al.*, 2004). Conifers were the most abundant trees (Stanley, 2009) in the Early Cretaceous [Aptian stage (Swisher *et al.*, 1999, 2002; Butler *et al.*, 2009; Sun *et al.*, 2011)], whereas angiosperms (i.e. flowering plants) radiated in the Latest Cretaceous (Soltis *et al.*, 2005; Stanley, 2009). Changes in floral composition may have spurred significant cranial and lower jaw shape changes within Ceratopsia, and within Ceratopsidae in particular, as a response to different dietary regimes. Mallon and Anderson (2014) suggest that the high number of micro-wear scratches in centrosaurines' teeth compared with chasmosaurines, was related to a more abrasive diet. Maiorino *et al.* (2015b) noted that the different mechanical behaviour of the triceratopsin lower jaw (and different morphology) might have been related to a different diet in centrosaurines and non-triceratopsin chasmosaurines.

Recent discoveries of new taxa and revisions of historically described taxa have increased the number of ceratopsian species and the cranial material available, with some taxa represented now by dozens of specimens. These new studies have increased the knowledge of the systematics and taxonomy of the group, along with their complex palaeobiogeography and evolutionary history (Sampson, 1995; Wolfe and Kirkland, 1998; Lambert *et al.*, 2001; Xu *et al.*, 2002, 2006, 2010a, 2010b; You *et al.*, 2005; Makovicky and Norell, 2006; Ryan, 2007; Sereno *et al.*, 2007, 2010; Wu *et al.*, 2007; Longrich, 2010, 2013; Sampson *et al.*, 2010, 2013; Farke *et al.*, 2011, 2014; Lee *et al.*, 2011; Fiorillo and Tykoski, 2012; Ryan *et al.*, 2012a, 2012b; Hedrick and Dodson, 2013; Wick and Lehman, 2013; Mallon *et al.*, 2014; Brown and Henderson, 2015; Evans and Ryan, 2015; Han *et al.*, 2015; Zheng *et al.*, 2015). This large dataset now allows the application of GM to skulls and lower jaws (both in lateral view) and a quantitative investigation of cranial and lower jaw shape variation within ceratopsians through time in a specific phylogenetic scenario.

In this context, we address three specific questions:

1. What is the range of shape variation in ceratopsian skulls and lower jaws?
2. Which clade possesses the most efficient feeding apparatus as measured by morphological integration between the skull and lower jaw?
3. What phenotypic rate shifts, if any, across the phylogeny characterize the evolution of ceratopsian cranial shape?

We address these questions in an attempt to understand better the tempo and mode of evolutionary history of Ceratopsia in relation to the angiosperm radiation event that occurred during the Cretaceous period as a potential mechanism for the elongation of the frill.

Institutional abbreviations

AMNH, American Museum of Natural History, New York, USA; **BHI**, Black Hills Institute of Geological Research, Hill City, South Dakota, USA; **CMN**, Canadian Museum of Nature, Ottawa, Ontario, Canada; **MOR**, Museum of the Rockies, Bozeman, Montana, USA; **OMNH**, Oklahoma Museum of Natural History, Norman, Oklahoma, USA; **TMP**, Royal Tyrrell Museum of Paleontology, Drumheller, Alberta, Canada; **USNM**, National Museum of Natural History, Smithsonian Institution, Washington DC, USA; **YPM**, Yale Peabody Museum of Natural History, New Haven, Connecticut, USA.

METHODS AND MATERIALS

We collected data from 121 ceratopsian skulls and 122 lower jaws in lateral view, both from original photos and published pictures. All ceratopsian species having a complete or nearly complete skull or lower jaw were included in the dataset. Fifty-five ceratopsian species are represented in the sample (10 centrosaurines, 11 non-triceratopsin chasmosaurines, 7 triceratopsins, 4 protoceratopsids, 8 psittacosaurids, 6 leptoceratopsids, 1 chaoyangsaurid, and several ceratopsians not belonging to a defined clade such as *Zuniceratops*, *Aquilops*, *Auroraceratops*, *Archaeoceratops* spp., *Liaoceratops*, *Yamaceratops*, and *Yinlong*). Tables S1 and S2 (www.evolutionary-ecology.com/data/3008Appendix) list the specimens, the number of individuals of each species, as well as the institutions from which the images were obtained. We followed a specific protocol for taking photographs of ceratopsian skulls and lower jaws in lateral view (following Marcus *et al.*, 2000 and Mullin and Taylor, 2002). We used a Canon 400D camera with an assembled Canon 17–85 mm lens. It was positioned on a tripod so that the lens was horizontal relative to the ground. The focusing points of the lens (arranged as a rhombus) were situated so that the two outer points of the major axis coincided with the external borders of the skull or lower jaw (3008Appendix, Fig. S1). Thus, any picture error due to a potential parallax effect was minimized or equal in every single photograph.

Geometric morphometrics

Geometric morphometrics is a suitable method to quantify morphological changes and to analyse phenotypic differences among taxa (Adams *et al.*, 2004; Zelditch *et al.*, 2012). Twenty-eight landmarks and 14 semi-landmarks in two dimensions were digitized on each skull in lateral view (Fig. 1 and Table S3), and 12 landmarks and 21 semi-landmarks were digitized on each lower jaw in lateral view (Fig. 2 and Table S3) using tpsDig2 v.2.17 software (Rohlf, 2013). Scale bars were used to scale each digitized specimen.

Taphonomic distortion can potentially be a major issue in a geometric morphometrics study. We addressed this problem in three ways. First, we excluded from the dataset incomplete skulls, skulls that had been damaged (often reconstructed using plaster), and specimens where distortion strongly altered the original shape. Specimens including AMNH 6443, AMNH 6417, AMNH 6251 (*Protoceratops andrewsi*), MOR 981 (*Torosaurus latus*), AMNH 5402 (*Chasmosaurus belli*), BHI 6441, YPM 1823 (*Triceratops horridus*), CMN 8798 (*Centrosaurus apertus*), TMP 2001.26.1 (*Albertaceratops nesmoi*), TMP 1986.126.01 (*Styracosaurus albertensis*), and TMP 1980.03.02 (*Pachyrhinosaurus canadensis*) were excluded from the sample because they were distorted, crushed dorso-ventrally or badly damaged. Second, we included in the dataset multiple specimens of the same taxon

where possible (e.g. *Centrosaurus apertus*, *Chasmosaurus belli*, *Pentaceratops sternbergi*, *Protoceratops andrewsi*, *Triceratops horridus*, and *Triceratops prorsus*). Third, we considered two separate subsets of landmarks to reduce the shape distortion related to the whole cranial morphology. We explored cranial shape changes focusing on the skull without frill and the frill alone (in lateral view) to determine whether the frill or the facial portion of the skull possesses anatomical traits (Fig. S2) useful to distinguish taxa within the ceratopsian clades (Dodson, 1993).

We digitized equally spaced semi-landmarks along outlines drawn on the specimens. Semi-landmarks are useful to capture morphological information of outlines where no homologous points can be detected. Curves or contours are assumed to be homologous among specimens (Bookstein *et al.*, 2002; Perez *et al.*, 2006). In a few cases, we used the function fixLMtps() in the 'Morpho' R package (Schlager, 2013) to estimate landmarks based on the three closest complete specimens to avoid errors during the digitization process. We decided to apply this procedure to a few moderately incomplete specimens only (e.g. *Anchiceratops ornatus* CMN 8535, *Pentaceratops sternbergi* OMNH 10165, *Triceratops horridus* USNM 1205, *Regaliceratops peterhewsi* TMP 2005.055.01) for which very small parts were missing (relative to the considered landmark configuration), whereas specimens that were too distorted or damaged were excluded as explained above.

Lower jaws are relatively flat bones and are usually less affected by postmortem distortion than more complicated three-dimensional (3D) structures such as crania. We digitized landmarks only on the lower jaw profile. The predentary was removed from the original configuration because it is often lost, damaged or restored with plaster. We also did not include the articular bone in the landmark configuration because it is often damaged or not visible in the lateral view.

Many specimens in the sample for basal ceratopsians (e.g. psittacosaurids, protoceratopsids) preserve an articulated lower jaw, whereas the surangular and angular are often found disarticulated in ceratopsids. Therefore, we again used the function fixLMtps() in the 'Morpho' R package (Schlager, 2013) to estimate landmarks for a few lower jaws (e.g. *Coronosaurus brinkmani* TMP 2002.68.166, *Einiosaurus procurvicornis* MOR 373-7-15-6-13, *Leptoceratops gracilis* AMNH 5205, *Triceratops* sp. USNM 8081) where those bones are missing.

Although a 2D geometry, compared with 3D structures such as vertebrate skulls, is undoubtedly a simplification and can obscure some morphological variation, we believe a 2D approach is justified based on the available dataset and for the purposes of looking at general trends across taxa. For this sample, it is currently difficult if not impossible to generate a number of 3D models. Specimen size, together with the inaccessibility of many specimens within exhibit mounts, prohibited photography from additional views (ventral and postero-dorsal) or the performance of computed tomography for many of the ceratopsian species under study. However, recent studies have nonetheless highlighted important findings on feeding biomechanics and lower jaw shape variation using a 2D approach (Neenan *et al.*, 2014; Maiorino *et al.*, 2015b).

Generalized Procrustes analysis [GPA (Bookstein, 1991)] implemented using the procSym() function in the 'Morpho' R package (Schlager, 2013) was used to analyse shape differences among species in the four different samples (i.e. entire skull in lateral view, skull without the frill and the frill alone in lateral view, and the lower jaw). GPA scales, aligns, and rotates each landmark configuration to the unit centroid size [CS = the square root of sum of squared differences between landmarks from their centroid (Bookstein, 1986)]. CS represents

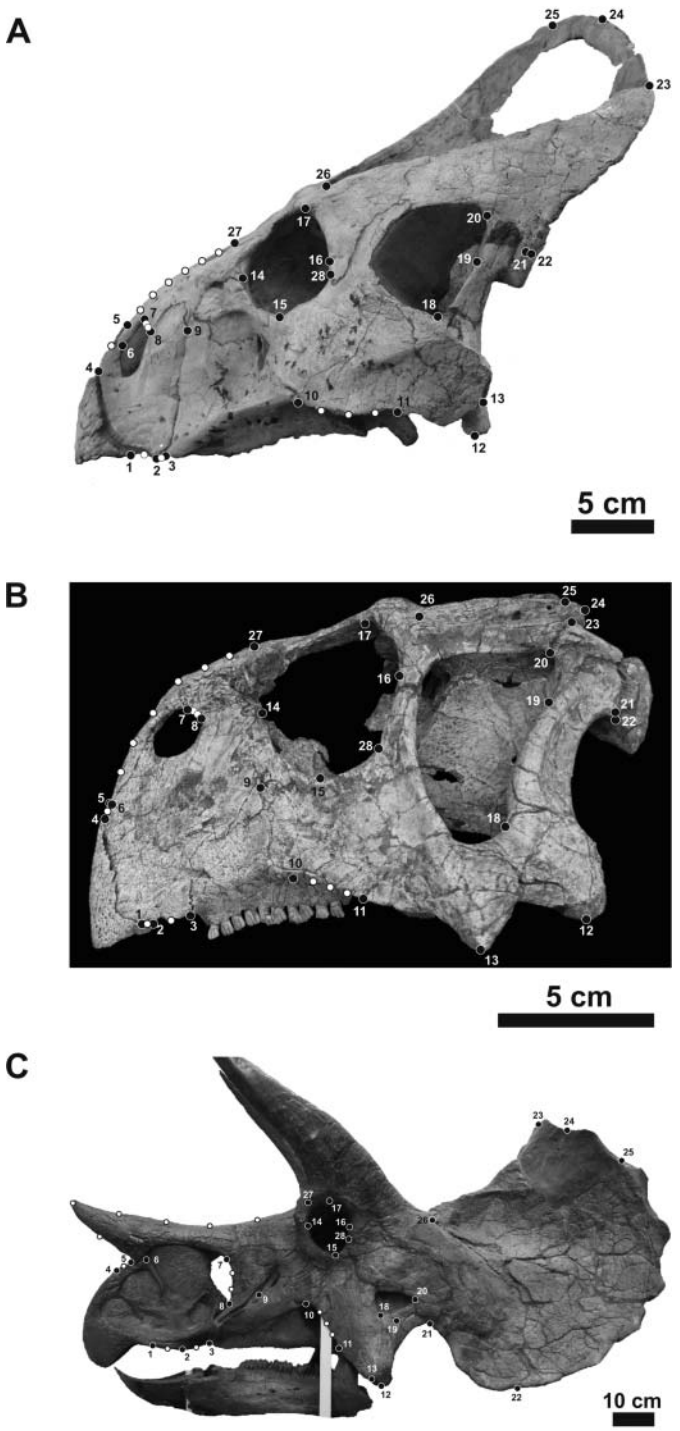
A
B
C
5 cm
5 cm
10 cm
Semi-landmark
Landmark

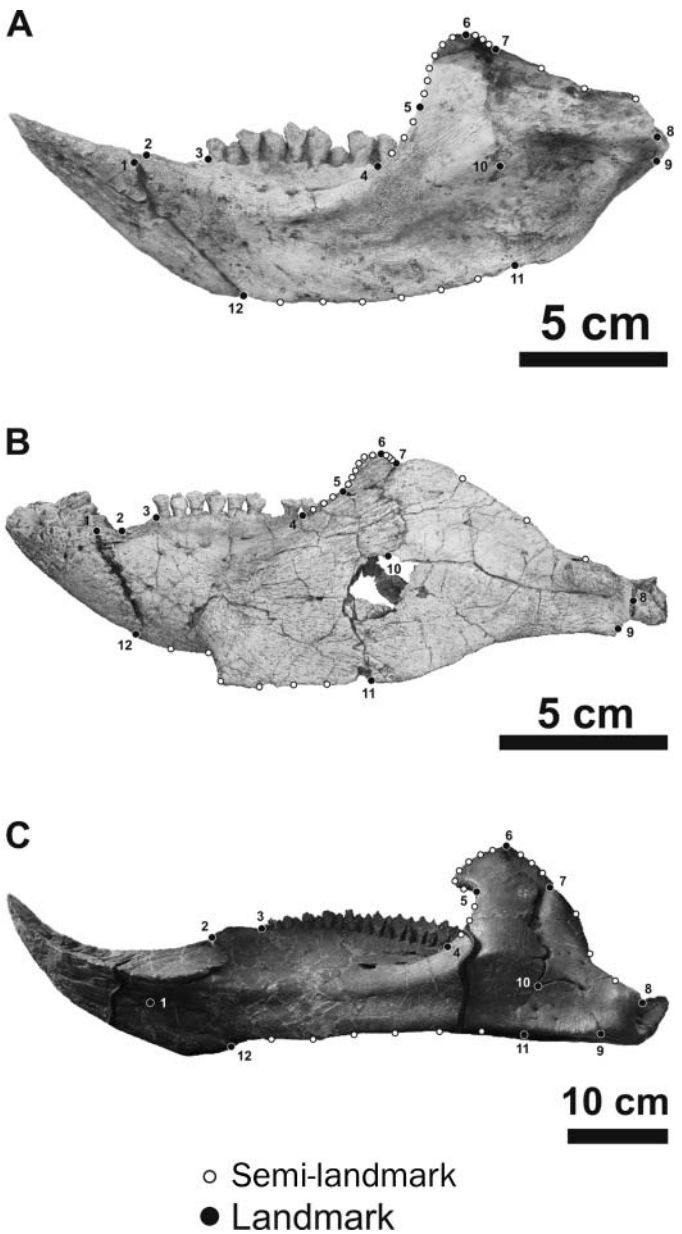

Fig. 1. (Opposite page) Landmarks and semi-landmarks configuration for the skull in lateral view. (A) *Protoceratops andrewsi* (AMNH 6429), (B) *Psittacosaurus major* (CAGS-IG-VD 004), (C) *Triceratops prorsus* (YPM 1822). See Table S3 in 3008Appendix for landmark definitions. The image of YPM 1822 (*T. prorsus*) is used with the permission of the Peabody Museum of Natural History, Yale University, New Haven, Connecticut, USA. All rights reserved.

Fig. 2. (Above) Landmarks and semi-landmarks configuration for the lower jaw in lateral view. (A) *Protoceratops andrewsi* (UALVP 49397), (B) *Psittacosaurus major* (CAGS-IG-VD 004), (C) *Centrosaurus apertus* (ROM 767). See Table S3 in 3008Appendix for landmark definitions.

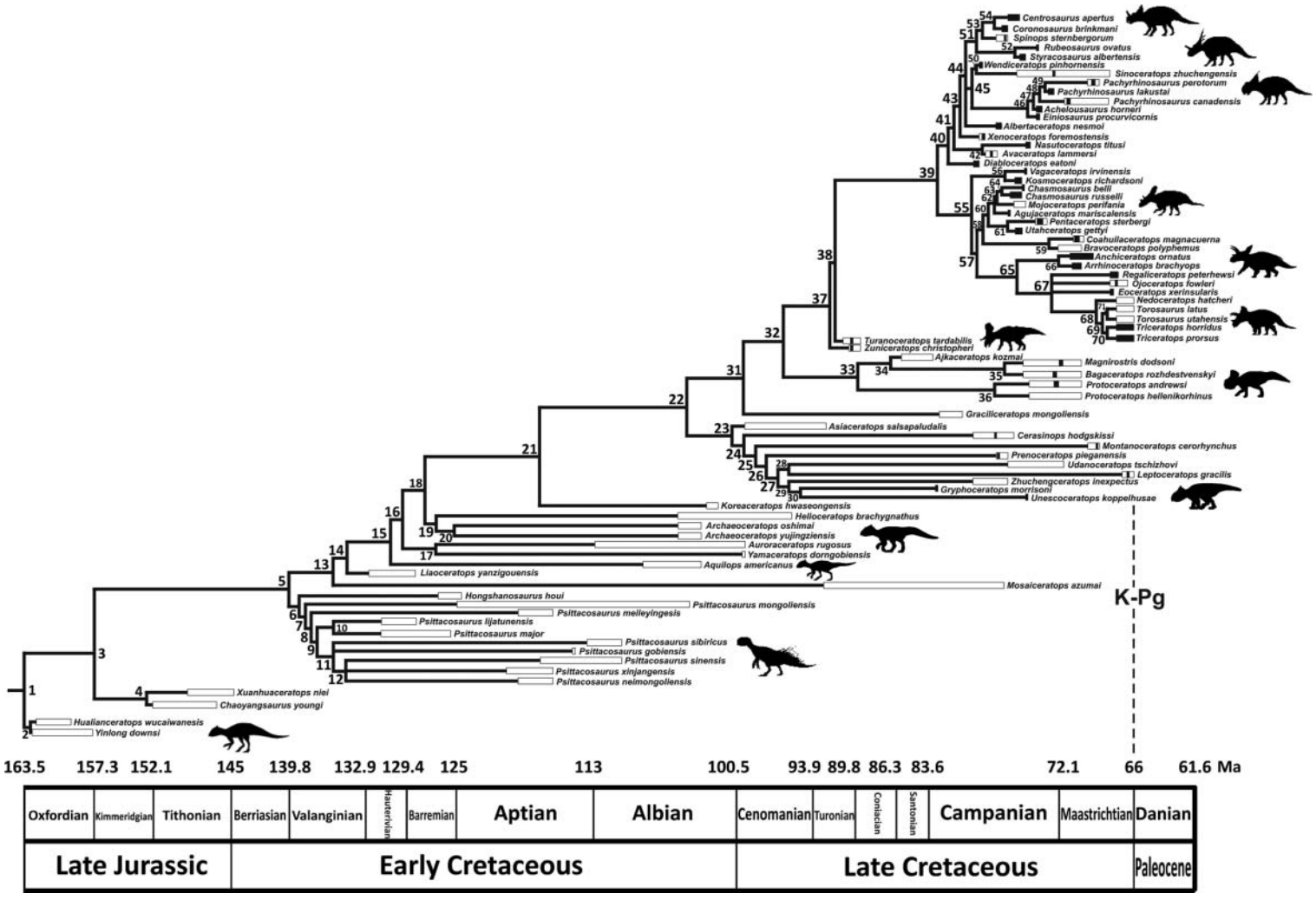
1 Hualianceratops wucaiwanesis
2 Yinlong downsi
3
4 Xuanhuaceratops niei
Chaoyangsaurus youngi
5
6 Hongshanosaurus houi
Psittacosaurus mongoliensis
7 Psittacosaurus melleyingesis
8 Psittacosaurus lijatunensis
9 Psittacosaurus major
10 Psittacosaurus sibiricus
11 Psittacosaurus gobiensis
12 Psittacosaurus sinensis
Psittacosaurus xinjangensis
Psittacosaurus neimongoliensis
13 Liaoceratops yanzigouensis
14 Aquilops americanus
15 Mosaiceratops azumai
16 Koreaceratops hwaseongensis
17 Helloceratops brachygnathus
18 Archaeoceratops oshimai
19 Archaeoceratops yujingziensis
20 Auroraceratops rugosus
Yamaceratops dorngobiensis
21
22 Asiaceratops salsapaludalis
23 Gracilicerato ps mongoliensis
24 Cerasinops hodgskissi
25 Montanoceratops cerorhynchus
26 Prenoceratops pieganensis
27 Udanoceratops tschizhovi
28 Leptoceratops gracilis
29 Zhuchengceratops inexpectus
30 Gryphoceratops morrisoni
Unescoceratops koppelhusae
31
32 Turanoceratops tardabilis
Zuniceratops christopheri
33
34 Ajkaceratops kozmai
35 Magnirostris dodsoni
Bagaceratops rozhdestvenskyi
36 Protoceratops andrewsi
Protoceratops hellenikorhinus
37
38
39
40 Centrosaurus apertus
41 Coronosaurus brinkmani
42 Spinops sternbergorum
43 Rubeosaurus ovatus
44 Styracosaurus albertensis
45 Wendiceratops pinhornensis
46 Sinoceratops zhuchengensis
47 Pachyrhinosaurus perotorum
48 Pachyrhinosaurus lakustai
Pachyrhinosaurus canadensis
Achelousaurus horneri
Einiosaurus procurvicornis
Albertaceratops nesmoi
Xenoceratops foremostensis
Nasutoceratops titusi
Avaceratops lammersi
Diabloceratops eatoni
Vagaceratops irvinensis
Kosmoceratops richardsoni
Chasmosaurus belli
Chasmosaurus russelli
Mojoceratops perifania
Agujaceratops mariscalensis
Penaceratops sternbergi
Utahceratops gettyi
Coahuilaceratops magnacuerna
Bravoceratops polyphemus
Anchiceratops ornatus
Arrhinoceratops brachyops
Regaliceratops peterhewsi
Ojoceratops fowleri
Eoceratops xerinsularis
Nedoceratops hatcheri
Torosaurus latus
Torosaurus utahensis
Triceratops horridus
Triceratops prorsus
K-Pg
163.5 157.3 152.1 145 139.8 132.9 129.4 125 113 100.5 93.9 89.8 86.3 83.6 72.1 66 61.6 Ma
Oxfordian
Kimmeridgian
Tithonian
Berriasian
Valanginian
Hauterivian
Barremian
Aptian
Albian
Cenomanian
Turonian
Coniacian
Santonian
Campanian
Maastrichtian
Danian
Late Jurassic
Early Cretaceous
Late Cretaceous
Paleocene

the individual size in all analyses. Rotation is achieved by comparison with a reference landmark configuration (usually the first specimen in the sample). Averaged shape variables per-species (Procrustes coordinates) from the aligned specimens were obtained and used in the subsequent analyses (Bookstein *et al.*, 1999; Mitteroecker and Bookstein, 2008). After GPA, principal components analysis (PCA) was performed on the averaged Procrustes coordinates per-species to identify orthogonal axes of maximal variation in the four datasets. This is a standard procedure in GM studies (Adams *et al.*, 2004; Claude, 2008; Piras *et al.*, 2010).

Phylogeny

We built a synthetic phylogenetic tree (Fig. 3) including all ceratopsian species using the software Mesquite v.2.75 (Maddison and Maddison, 2011), following the most recent published cladistic analyses.

We followed Sampson *et al.* (2010, 2013), Evans and Ryan (2015), and Brown and Henderson (2015) regarding the affinities within Chasmosaurinae and Centrosaurinae. Lambert *et al.* (2001), Ösi *et al.* (2010), Sampson and Loewen (2010), Ryan *et al.* (2012a), and Farke *et al.* (2014) were considered for the relationships within Protoceratopsidae. For the phylogenetic relationships within Leptoceratopsidae, we followed Nessov *et al.* (1989), Nessov (1995), Chinnery (2004b), Chinnery and Horner (2007), Ryan *et al.* (2012a), and Farke *et al.* (2014), whereas the relationships within Psittacosauridae are based on You *et al.* (2003), You and Xu (2005), Lucas (2006), Sereno (2010), and Sereno *et al.* (2010).

We calibrated branch lengths in millions of years (Ma) based on the stratigraphic occurrences in the fossil record. Further details about the additional literature sources upon which we built the synthetic phylogeny are provided in Tables S4 and S5 (3008Appendix).

Morphological integration

Some studies have addressed the morphological integration between different modular regions within Mammalia, Reptilia, and Aves (Atchley *et al.*, 1982; Atchley and Hall, 1991; Cheverud *et al.*, 1991, 1997, 2004; Badyaev and Foresman, 2000, 2004; Klingenberg and Leamy, 2001; Klingenber *et al.*, 2001, 2003, 2004; Leamy *et al.*, 2002; Ehrich *et al.*, 2003; Cheverud, 2004; Badyaev *et al.*, 2005; Polly, 2005; Márquez, 2008; Zelditch *et al.*, 2009; Klingenberg and Marugán-Lobón, 2013; Piras *et al.*, 2013) but little has been conducted within non-avian Dinosauria (Maiorino *et al.*, 2013b).

Here, we compare the degree of morphological integration among clades, between the entire skull and lower jaw, and between the skull without frill, the frill alone, and the lower jaw. We used the RV coefficient (Escoufier, 1973) as a metric of covariation between various sets of shape variables using the average values per-species to avoid errors due to pseudo-replication of data. In a recent paper, Fruciano and colleagues (2013) showed that the RV

Fig. 3. Synthetic phylogenetic tree with all ceratopsian species considered valid in this study. See text and Tables S4 and S5 in 3008Appendix for details about topology and branch length calibration. Thicker lines indicate the stratigraphic range of taxa. Black bars indicate confident stratigraphic occurrence, whereas white bars indicate less confidence. *Psittacosaurus* image by J. Headden; *Zuniceratops* and *Einiosaurus* images by Nobu Tamura, modified by T. Michael Keesey; *Archaeoceratops*, *Protoceratops*, *Leptoceratops*, *Aquilops*, *Pachyrhinosaurus*, *Centrosaurus*, *Styracosaurus*, *Yinlong*, and *Chasmosaurus* by Andrew A. Farke; *Triceratops* by Raven Amos. All images except *Zuniceratops* (in public domain) are licensed under Creative Commons Attribution 3.0 licence.

coefficient depends on sample size. They suggested a rarefaction procedure to obtain sample-size-corrected RV values. The RV coefficient has been calculated using the function rarefrvst( ), developed by Dr. Paolo Piras, which takes into account sample size.

The RV coefficient is analogous to R-squared in the univariate case (Claude, 2008). The equation for calculating RV therefore represents the amount of covariation scaled by the amount of variation within the two sets of variables, which is analogous to the calculation of the correlation coefficient between two variables (Klingenberg, 2009). RV may take any value from 0 to 1.

Partial least square (PLS) analysis was performed to visualize the covariation between the skull (in lateral view, skull without frill and the frill alone) and lower jaw at the macroevolutionary scale (Meloro *et al.*, 2011; Meloro and Slater, 2012; Piras *et al.*, 2013). This technique identifies pairs of vectors (singular warps) that maximize the covariation between two blocks of multivariate data (Rohlf and Corti, 2000) that here are represented by shape variables of the skull and lower jaw, respectively. These vectors are useful for describing whatever pattern of covariation exists between the two sets of shape variables. Moreover, PLS treats variable blocks as symmetrical, without assuming a dependence–independence relationship.

Lastly, we calculated the degree of morphological integration between the skull without frill and the frill alone (in lateral view) among clades as well as the RV coefficient, using the part–whole approach (Marquez, 2008; Maiorino *et al.*, 2013b), in order to assess which part (between the frill and the skull without frill) drives the change of shape of the entire skull.

Linear models and comparative methods

Comparative data are rarely independent in biology, as assumed in standard regressions. Taking phylogeny into account in regressions permits a reduction in the standard error due to the non-independence of data related to a shared ancestry over a model that neglects phylogeny (Felsenstein, 1985; Garland, 1992; Garland *et al.*, 2005). Thus, we first tested for significant phylogenetic signal in size (CS) using the function phylosig( ) in the 'phytools' R package (Revell, 2012). Shape consists of multivariate data, so we used the function physignal( ) in the 'geomorph' R package (Adams and Otarola-Castillo, 2013) to estimate the degree of phylogenetic signal in shape data for a given phylogenetic tree.

We examined relationships between shape (as dependent; averaged per-species values) and size (as independent; averaged per-species values) variables using an ordinary least square (OLS) linear regression in order to explore the influence of allometry among and within clades. Because shape is multivariate and for the sake of visualization, we used canonical correlation analysis (CCA) to plot the regression score representing shape against the independent variable size (CS). Moreover, to ensure those associations were not affected by a phylogenetic effect, we used the phylogenetic generalized least squares [PGLS (Rohlf, 2001, 2006)] regression. This method is equivalent to the phylogenetic independent contrasts (PICs) proposed by Felsenstein (1985).

We then tested for differences in shape and size among six distinct clades (non-triceratopsin Chasmosaurinae, Triceratopsini, Centrosaurinae, Protoceratopsidae, Leptoceratopsidae, and Psittacosauridae) identifiable in the phylogeny. We performed pair-wise comparisons on size using a non-parametric permuted analysis of variance (perANOVA) and on shape using a non-parametric permuted multivariate analysis of variance (perMANOVA). We performed those tests using the function adonis( ) in the 'vegan' R

package (Oksanen *et al.*, 2011), which manages unequal sample sizes (1000 permutations). Several ceratopsian taxa, including *Zuniceratops christopheri*, *Aquilops americanus*, *Auroraceratops rugosus*, *Archaeoceratops* spp., *Liaoceratops yanzigouensis*, and *Yamaceratops dorngobiensis*, were excluded from the analyses because they do not belong to any particular evolutionary radiation within Ceratopsia. Chaoyangsauridae and the *Yinlong* + *Hualianceratops* group were excluded because these clades have only one species (*Chaoyangsaurus youngi* and *Yinlong downsi*, respectively) in the sample.

Lastly, we also regressed the cranial averaged shape values and Cretaceous angiosperm occurrences (data from Butler *et al.*, 2009) to investigate the relationship between shape and angiosperm radiation. Basically, we associated the mid-point of the stratigraphic range for each ceratopsian in our sample to the age-correspondent global angiosperm occurrence (expressed as a percentage). We performed this test, using an OLS linear model (function adonis( ) in the 'vegan' R package), to explore the potential relationships between shape and the angiosperm radiation event that occurred during the Cretaceous period.

Phenotypic evolutionary rates

The relationships between taxa are described in phylogenetic trees, which also can depict the tempo and mode of evolution among several lineages (Thomas and Freckleton, 2012). Identifying and estimating phenotypic evolutionary shifts across the phylogeny introduces a new datum in revealing the mechanisms that generated differences in the geographic and taxonomic distribution of related organisms through time (Adams *et al.*, 2009; Thomas and Freckleton, 2012). The 'MOTMOT' R package provides a useful tool to investigate if any changes in the evolutionary rates of univariate or multivariate metrics occur in the internal nodes of a given phylogeny (O'Meara *et al.*, 2006; Thomas *et al.*, 2009; Thomas and Freckleton, 2012). Evolutionary rates of ceratopsian cranial (skull in lateral view, skull without frill, and frill alone) and lower jaw shape mean values have been tested across the phylogeny, identifying internal nodes where a particular shift of a phenotypic trait occurs. Furthermore, we compared evolutionary rates for shape among clades by means of the function transformPhylo.ML( ) in the 'MOTMOT' R package using maximum-likelihood evaluation.

RESULTS

Geometric morphometrics

Cranial shape variation within Ceratopsia

The first 11 principal components of the PCA, performed on the skulls in lateral view, together explain 95% of overall shape variance. Figure 4A shows the relationship between PC1 (59.69% of overall shape variance) and PC2 (11.07% of overall shape variance) while Fig. 4B shows the relationship between PC1 and PC3 (7.16% of overall shape variance). Negative PC1 values are associated with a massive and long skull bearing a high and caudodorsally expanded parieto-squamosal complex, small orbit (proportional to the size of the rest of the skull), a long snout with a rostrally expanded premaxilla-maxilla complex, rostral tip of the supratemporal fenestra located above the infratemporal fenestra, the presence of a nasal horn, and lower tip of the quadrate shifted forward with respect to the tip of the jugal. This morphology is chasmosaurine-like. Positive PC1 values are associated

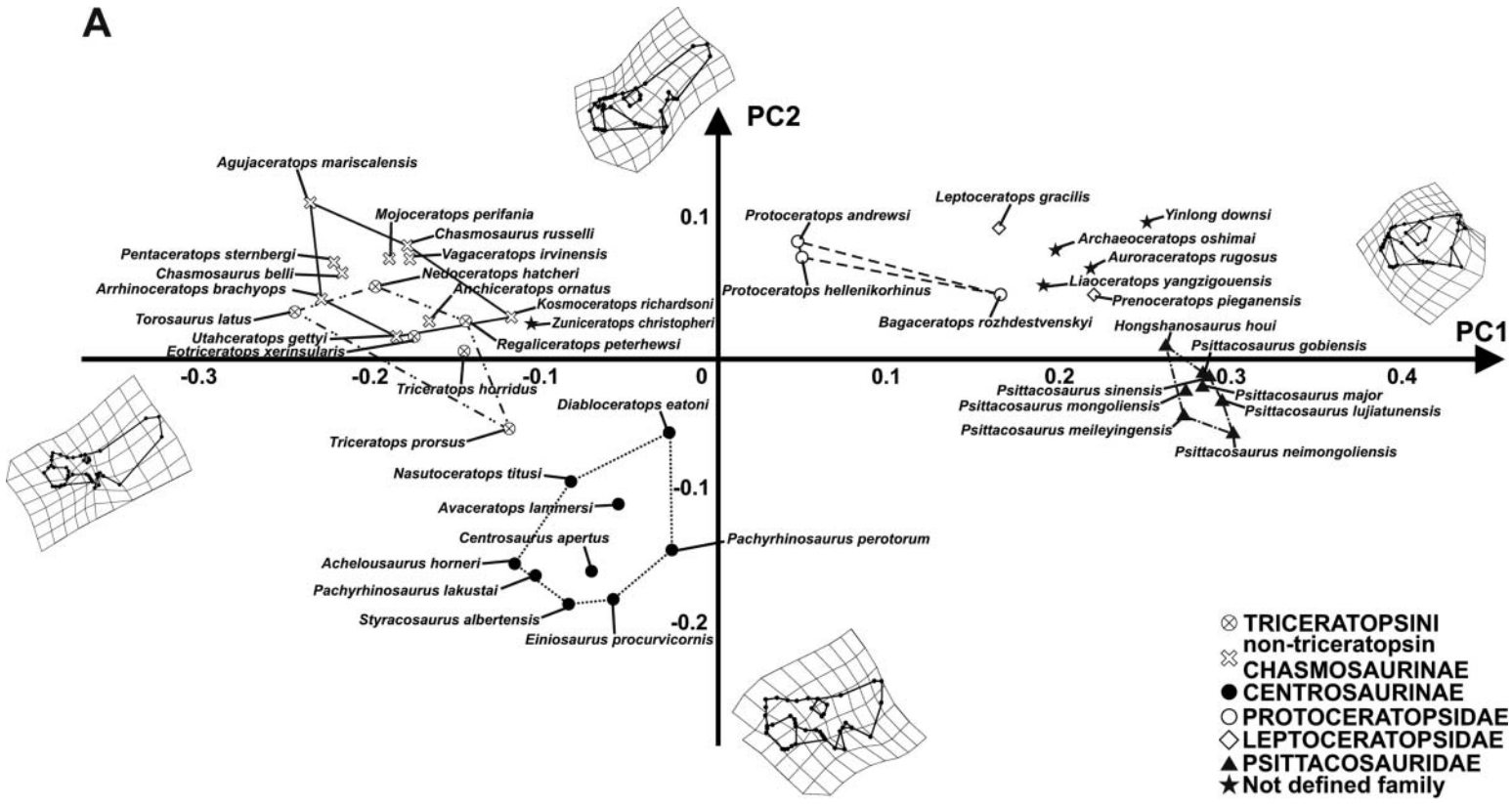
A
PC2
PC1
0.1
-0.1
-0.2
-0.3
-0.2
-0.1
0
0.1
0.2
0.3
0.4
Agujaceratops mariscalensis
Mojoceratops perifania
Chasmosaurus russelli
Vagaceratops irvinensis
Pentaceratops sternbergi
Chasmosaurus belli
Nedoceratops hatcheri
Arrhinoceratops brachyops
Anchiceratops ornatus
Kosmoceratops richardsoni
Torosaurus latus
Zuniceratops christopheri
Utahceratops gettyi
Regaliceratops peterhewsi
Eotriceratops xerinsularis
Triceratops horridus
Triceratops prorsus
Diabloceratops eatoni
Nasutoceratops titusi
Avaceratops lammersi
Centrosaurus apertus
Pachyrhinosaurus perotorum
Achelousaurus horneri
Pachyrhinosaurus lakustai
Styracosaurus albertensis
Einiosaurus procurvicornis
Protoceratops andrewsi
Leptoceratops gracilis
Yinlong downsi
Archaeoceratops oshimai
Auroraceratops rugosus
Protoceratops hellenikorhinus
Liaoceratops yangzigouensis
Prenoceratops pieganensis
Bagaceratops rozhdestvenskyi
Hongshanosaurus houi
Psittacosaurus gobiensis
Psittacosaurus sinensis
Psittacosaurus major
Psittacosaurus mongoliensis
Psittacosaurus lujiatunensis
Psittacosaurus meileyingensis
Psittacosaurus neimongoliensis
TRICERATOPSINI
non-triceratopsin CHASMOSAURINAE
CENTROSAURINAE
PROTOCERATOPSIDAE
LEPTOCERATOPSIDAE
PSITTACOSAURIDAE
Not defined family

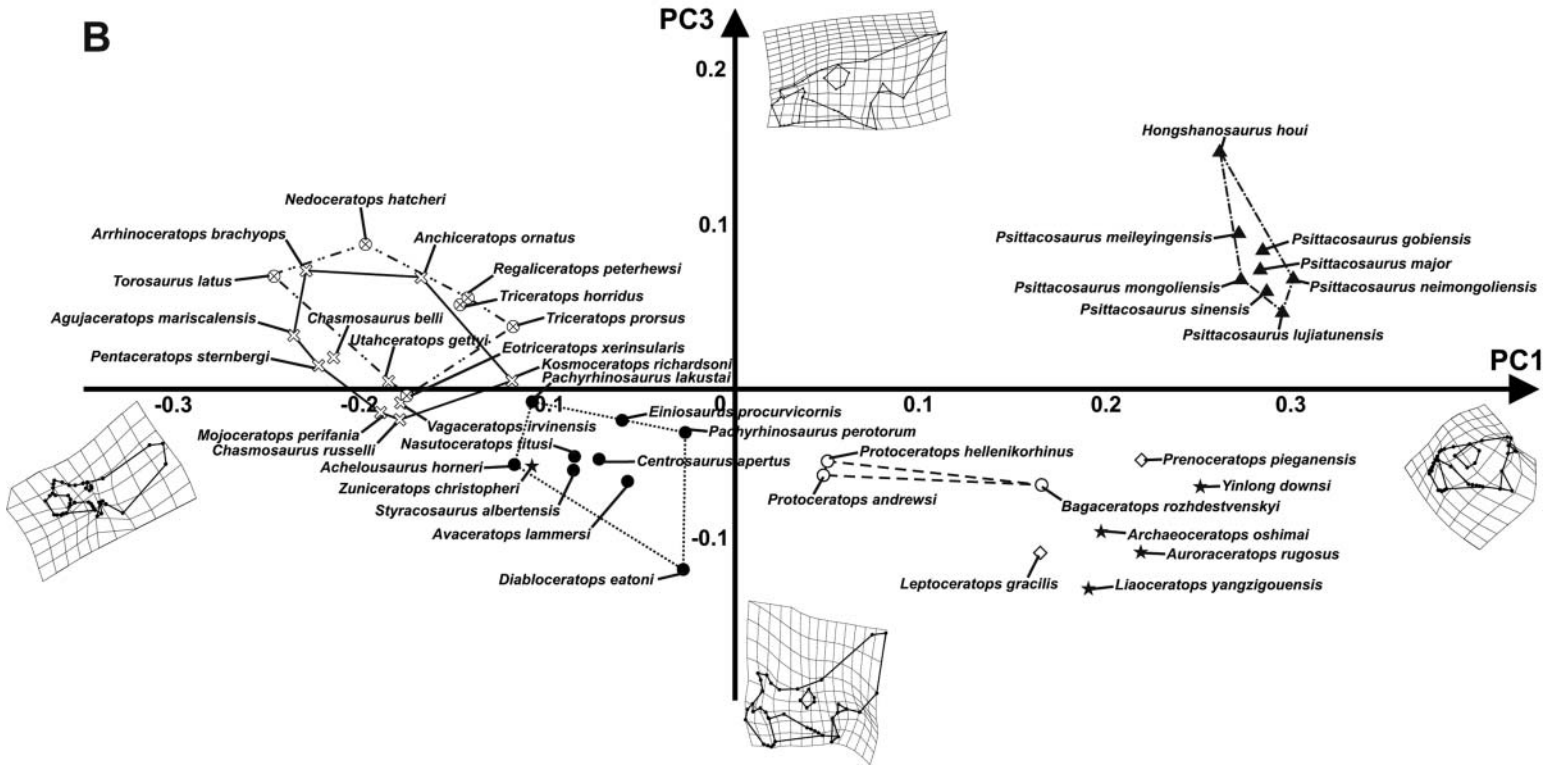

Fig. 4. (A) Relationship between PC1 and PC2 of cranial shape. (B) Relationship between PC1 and PC3 of cranial shape. The continuous line represents non-triceratopsin Chasmosaurinae morphospace. The dotted line represents Centrosaurinae morphospace. The double dot-dashed line represents Triceratopsini morphospace. The dashed line represents Protoceratopsidae morphospace and the dot-dashed line represents Psittacosauridae morphospace.

with a short and deep skull, with a short parieto-squamosal complex, absence of a nasal horn, large orbit (proportional to the size of the rest of the skull), a premaxilla-maxilla complex that is short and dorsally expanded, rostral tip of the supratemporal fenestra located above the caudal tip of the orbit, an expanded jugal, and lower tip of the quadrate shifted backward with respect to the tip of the jugal. This morphology is typical of psittacosaurids. A centrosaurine-like skull is associated with negative PC2 values. The skull has a moderately caudally developed frill, a nearly squared squamosal, nasal horn, lower tip of the quadrate shifted backward with respect to the jugal tip, short circumnarial region and short maxilla, and rostral tip of the supratemporal fenestra located above the infratemporal fenestra. By contrast, a protoceratopsid-like skull is associated with positive PC2 values. The skull is short with a moderately caudo-dorsally elongated frill, rostral tip of the supratemporal fenestra located almost above the caudal tip of the orbit, a moderately pronounced nasal horn, an infratemporal fenestra rising to the same height as the orbit, lower tip of the quadrate shifted forward with respect of the jugal tip, a short and dorsally developed premaxilla, and a premaxilla-maxilla upper contact rising to the same height as the lower tip of the orbit.

At positive PC3 values the skull has a moderately elongated snout, a short nasal horn, a caudally expanded frill, a rostral tip of the supratemporal fenestra located almost above the tip of the jugal, and lower edge of the quadrate located posterior to the jugal tip. At negative PC3 values, the skull bears a long nasal horn, short and deep circumnarial region, a dorsally expanded frill, and lower tip of the quadrate shifted forward relative to the jugal tip.

In summary, ceratopsids vary mainly along negative PC1 values, whereas protoceratopsids, basal neoceratopsians, and psittacosaurids vary mainly along positive PC1 values. Within Ceratopsidae, non-triceratopsin chasmosaurines vary along negative PC1 values and positive PC2 values, whereas triceratopsins vary along negative PC1 values and positive PC2 and PC3 values. Triceratopsin morphospace overlaps non-triceratopsin chasmosaurine morphospace, indicating a similar cranial morphology. Centrosaurines vary along negative PC1, PC2, and PC3 values.

Leptoceratopsid taxa (*Leptoceratops gracilis* and *Prenoceratops pieganensis*) are placed at high positive PC1 values, close to basal ceratopsian taxa (*Auroraceratops*, *Archaeoceratops*, *Liaoceratops*, and *Yinlong*). Figure S3 shows the 3D relationship between PC1, PC2, and PC3.

Lower jaw shape variation within Ceratopsia

The first nine principal components of the PCA, performed on the lower jaws in lateral view, together explain 95% of overall shape variance. Figure 5A shows the relationship between PC1 (49.92% of overall shape variance) and PC2 (17.06% of overall shape variance), while Fig. 5B shows the variation between PC1 and PC3 (9.54% of overall shape variance). Negative PC1 values are associated with a ceratopsid-like lower jaw, having a long and slender dentary, a strongly dorsally developed coronoid process, long tooth row, short angular, and dorso-ventrally elongated surangular. Positive PC1 values are associated with a psittacosaurid-like lower jaw, having a short and massive dentary, short tooth row, short coronoid process and long, caudally elongated surangular-angular complex. At positive PC2 values, the lower jaw has a moderately elongated and deep dentary, dorsally developed coronoid process, short and dorso-ventrally elongated angular and surangular. This morphology is typical of leptoceratopsids. At negative PC2 values, the lower jaw has a long and slender dentary, short coronoid process, long tooth row, and long and slender, caudally

elongated angular and surangular. This morphological arrangement is typical of *Yinlong downsi*. Negative PC3 values are associated with a lower jaw having a short and massive dentary, short tooth row, a dorsally developed coronoid process, short angular, and a caudo-ventrally elongated surangular, whereas at positive PC3 values the lower jaw is long and slender with a convex ventral edge, bearing a moderately dorsally elongated coronoid process, long tooth row, and a caudally expanded angular-surangular complex.

In summary, ceratopsids vary mainly along negative PC1 values. Within Ceratopsidae there is no clear differentiation among species, and all taxa appear to share the same general morphological structure. Leptoceratopsids vary along positive PC1 and PC2 values. Protoceratopsids vary mainly along positive PC1 and PC2 values. Psittacosaurids vary along high positive PC1 values and negative PC2 and PC3 values. All taxa cluster together in the morphospace with no clear distinction among species. The basal ceratopsian *Yinlong downsi* is clearly separated from the other ceratopsian taxa in the morphospace at extreme negative PC2 values and positive PC1 values. *Zuniceratops* lies close to ceratopsid morphospace, suggesting a similar lower jaw shape. Figure S4 shows the 3D relationship between PC1, PC2, and PC3.

For the frill and skull without frill shape variance, see text and Figs. S5, S6, S7, and S8 in 3008Appendix.

Allometric shape variation

We performed an OLS regression between multivariate shape (dependent variable) and size (independent variable, quantified by centroid size) for the entire sample to explore evolutionary allometry within Ceratopsia. Table 1 reports R^2 and P-values for the pooled datasets and for the individual clades under investigation for overall cranial shape, separate modules (i.e. skull without frill and frill alone), and lower jaws. PGLS was performed only on the pooled datasets. All linear regressions performed on the pooled datasets are significant, whereas the linear regressions performed within each clade are not. The PGLS result is not significant, indicating that the association between shape and size is influenced by the phylogenetic relationships. These results suggest the absence of evolutionary allometry within Ceratopsia as well as within each clade studied here.

Figure 6 shows the morphological cranial changes associated with size (CS). At high CS values the skull is chasmosaurine-like, having a caudo-dorsally expanded frill, a triangular squamosal, long and low facial portion of the skull with a long maxilla and premaxilla, small orbit, a well-developed nasal horn rostrally oriented, and ventral tip of the quadrate located forward of the jugal tip. At low CS values the skull is short and deep, bearing a short facial portion with short premaxilla and maxilla, large orbit, no nasal horn, an incipient frill with a short squamosal, large infratemporal fenestra, and ventral tip of the quadrate located behind the jugal tip. This morphological arrangement is typical of psittacosaurids.

Figure 7 shows the relationship between changes in lower jaw shape and CS values. At high CS values the lower jaw is long and slender, bearing a long tooth row, a long and slender dentary, a strongly developed coronoid process, and a short angular-surangular complex. This morphology is typical of ceratopsids. At low CS values the lower jaw is psittacosaurid-like. The dentary is short and massive, the tooth row is short as well as the coronoid process, and the angular and surangular are caudally elongated.

For the allometric shape variance of frills and skulls without frill, see text and Figs. S9 and S10 in 3008Appendix.

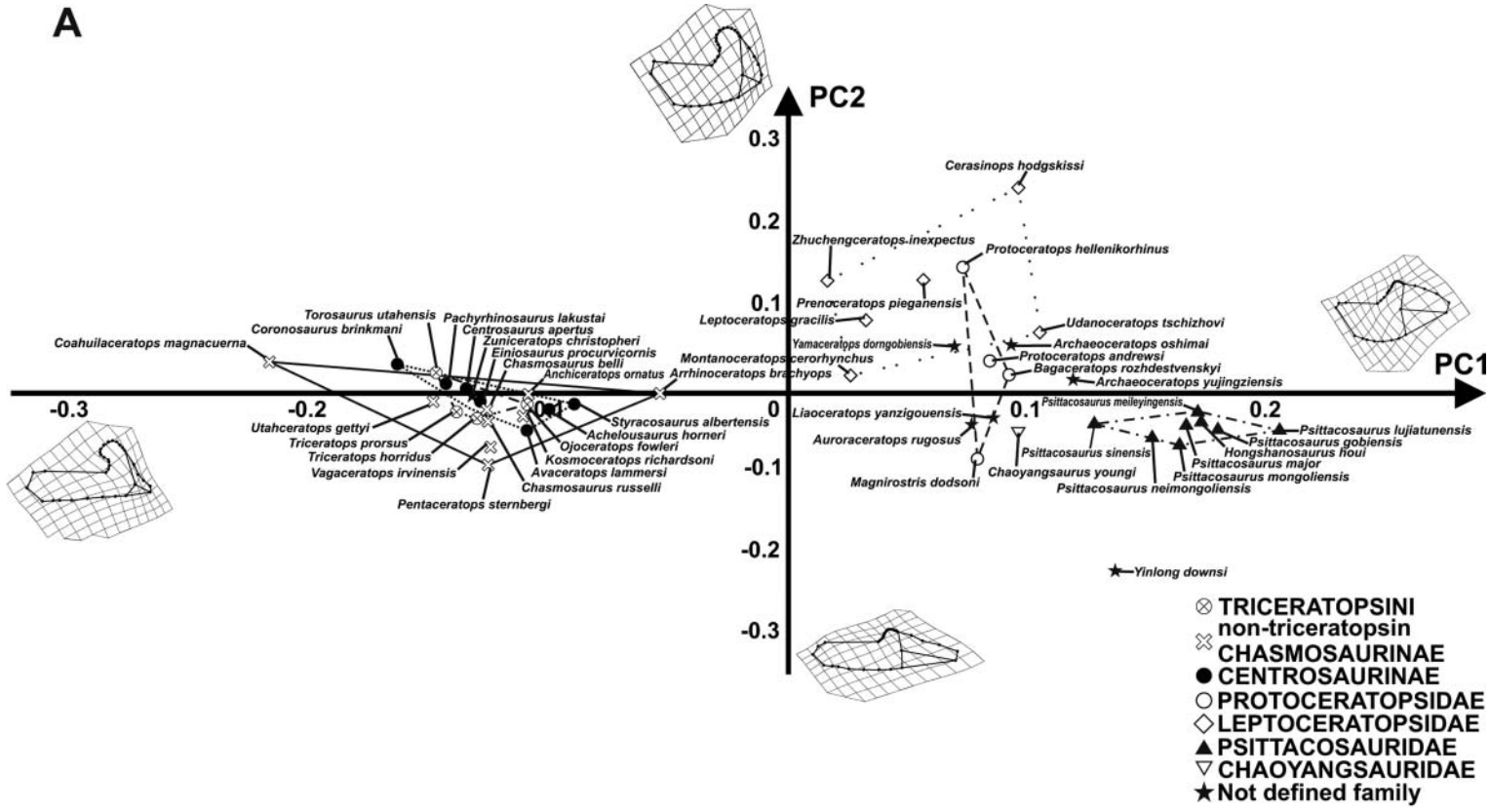
A
PC2
PC1
0.3
0.2
0.1
0
-0.1
-0.2
-0.3
-0.3
-0.2
-0.1
0
0.1
0.2
Cerasinops hodgskissi
Zhuchengceratops inexpectus
Protoceratops hellenikorhinus
Prenoceratops pieganensis
Leptoceratops gracilis
Udanoceratops tschizhovi
Yamaceratops dorngobiensis
Archaeoceratops oshimai
Montanoceratops cerorhynchus
Protoceratops andrewsi
Arrhinoceratops brachyops
Bagaceratops rozhdestvenskyi
Archaeoceratops yujingziensis
Psittacosaurus meileyingensis
Liaoceratops yanzigouensis
Auroraceratops rugosus
Psittacosaurus lujiatunensis
Psittacosaurus gobiensis
Hongshanosaurus houi
Psittacosaurus sinensis
Psittacosaurus major
Chaoyangsaurus youngi
Psittacosaurus mongoliensis
Magnirostris dodsoni
Psittacosaurus neimongoliensis
Torosaurus utahensis
Pachyrhinosaurus lakustai
Coronosaurus brinkmani
Centrosaurus apertus
Coahuilaceratops magnacuerna
Zuniceratops christopheri
Einiosaurus procurvicornis
Chasmosaurus belli
Anchiceratops ornatus
Styracosaurus albertensis
Achelousaurus horneri
Utahceratops gettyi
Ojoceratops fowleri
Triceratops prorsus
Kosmoceratops richardsoni
Triceratops horridus
Avaceratops lammersi
Vagaceratops irvinensis
Chasmosaurus russelli
Pentaceratops sternbergi
Yinlong downsi
TRICERATOPSINI
non-triceratopsin CHASMOSAURINAE
CENTROSAURINAE
PROTOCERATOPSIDAE
LEPTOCERATOPSIDAE
PSITTACOSAURIDAE
CHAOYANGSAURIDAE
Not defined family

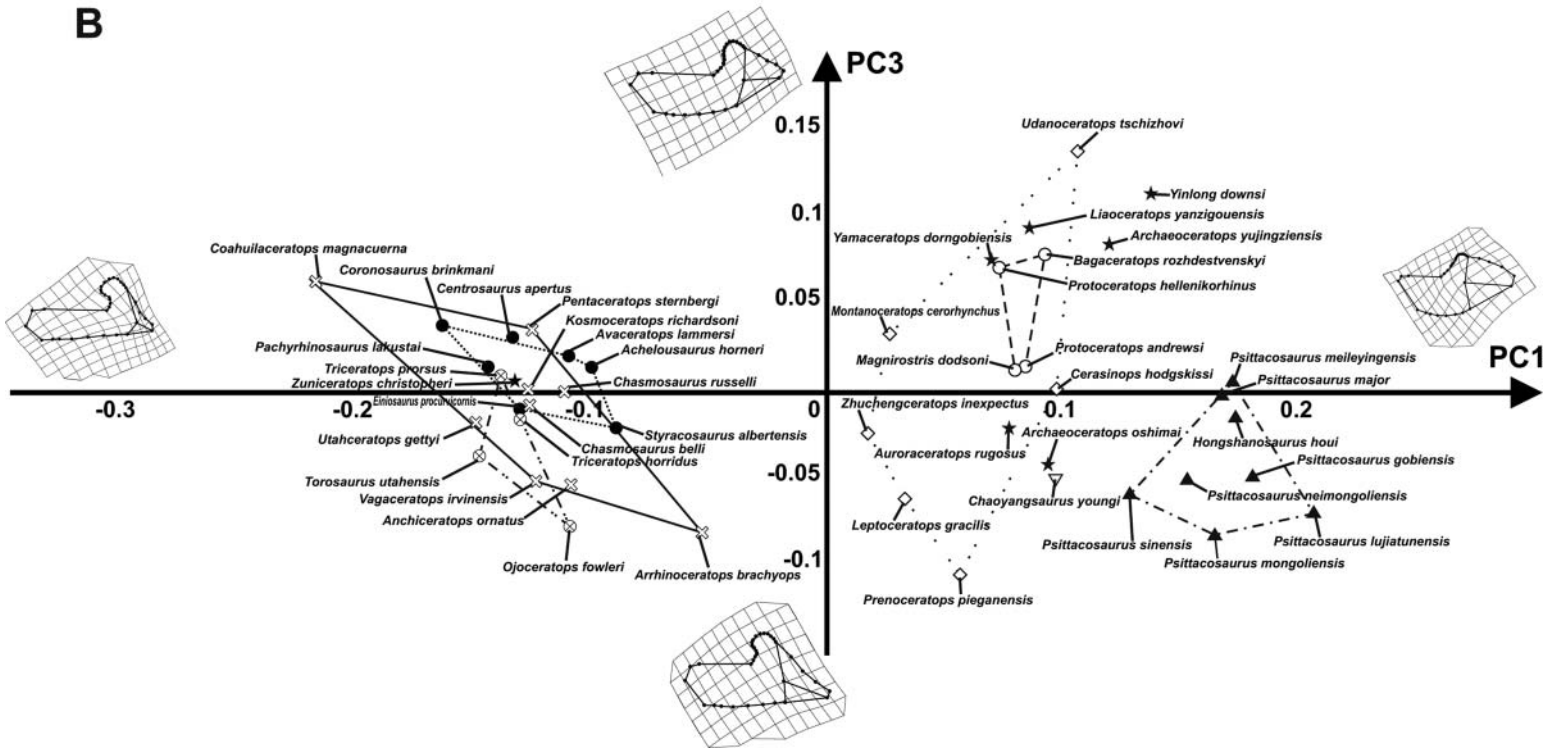

Fig. 5. (A) Relationship between PC1 and PC2 of lower jaw shape. (B) Relationship between PC1 and PC3 of lower jaw shape. The dotted line represents Centrosaurinae morphospace. The continuous line represents non-triceratopsin Chasmosaurinae morphospace. The double dot-dashed line represents Triceratopsini morphospace. The dashed line represents Protoceratopsidae morphospace. The double dotted line represents Leptoceratopsidae morphospace and the dot-dashed line represents Psittacosauridae morphospace.

Table 1. OLS models for pooled datasets and individual clades for shape–size relationship, and PGLS models for pooled samples

Shape	Centroid size
Skulls	
Pooled sample	$\mathbf{R^2 = 0.500, P = 0.0.001}$
Triceratopsini	$R^2 = 0.292$, $P = 0.143$
N-t Chasmosaurinae	$R^2 = 0.051$, $P = 0.944$
Centrosaurinae	$R^2 = 0.121$, $P = 0.480$
Protoceratopsidae	$R^2 = 0.707$, $P = 0.33$
Psittacosauridae	$R^2 = 0.081$, $P = 0.788$
Skulls without the frill	
Pooled sample	$\mathbf{R^2 = 0.322, P = 0.001}$
Triceratopsini	$R^2 = 0.213$, $P = 0.408$
N-t Chasmosaurinae	$R^2 = 0.091$, $P = 0.611$
Centrosaurinae	$R^2 = 0.105$, $P = 0.602$
Protoceratopsidae	$R^2 = 0.316$, $P = 0.416$
Leptoceratopsidae	$R^2 = 0.572$, $P = 0.5$
Psittacosauridae	$R^2 = 0.099$, $P = 0.647$
Frills	
Pooled sample	$\mathbf{R^2 = 0.514, P = 0.001}$
Triceratopsini	$R^2 = 0.279$, $P = 0.172$
N-t Chasmosaurinae	$R^2 = 0.057$, $P = 0.771$
Centrosaurinae	$R^2 = 0.132$, $P = 0.396$
Protoceratopsidae	$R^2 = 0.845$, $P = 0.166$
Leptoceratopsidae	$R^2 = 0.753$, $P = 0.166$
Psittacosauridae	$R^2 = 0.068$, $P = 0.854$
Lower jaws	
Pooled sample	$\mathbf{R^2 = 0.365, P = 0.001}$
Triceratopsini	$R^2 = 0.199$, $P = 0.666$
N-t Chasmosaurinae	$R^2 = 0.159$, $P = 0.236$
Centrosaurinae	$R^2 = 0.218$, $P = 0.240$
Protoceratopsidae	$R^2 = 0.213$, $P = 0.625$
Leptoceratopsidae	$R^2 = 0.213$, $P = 0.336$
Psittacosauridae	$R^2 = 0.149$, $P = 0.410$
PGLS	
Skulls	$P = 0.532$
Skulls with frill excluded	$P = 0.554$
Frills	$P = 0.204$
Lower jaws	$P = 0.159$

Note: Statistically significant results ($P < 0.05$) are indicated in **bold**. N-t Chasmosaurinae = Non-triceratopsin Chasmosaurinae.

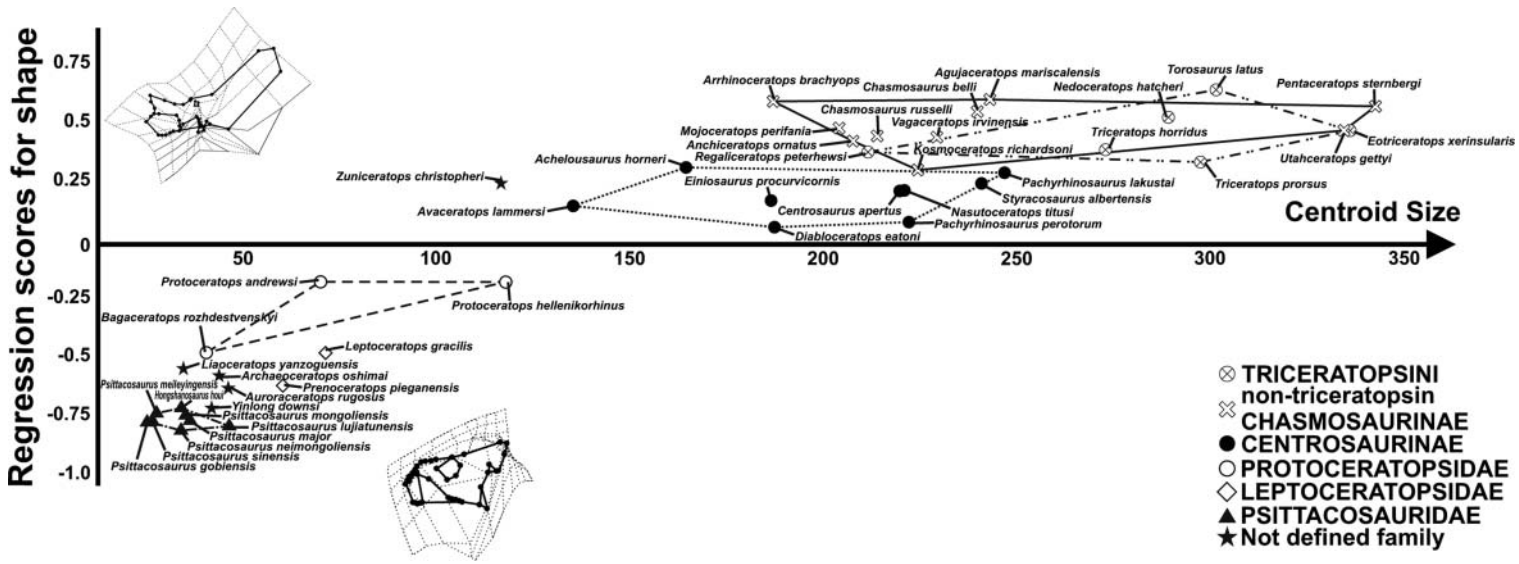

Fig. 6. Relationship between shape of skull and size. The continuous line represents non-triceratopsin Chasmosaurinae morphospace. The dotted line represents Centrosaurinae morphospace. The double dot-dashed line represents Triceratopsini morphospace. The dashed line represents Protoceratopsidae morphospace and the dot-dashed line represents Psittacosauridae morphospace.

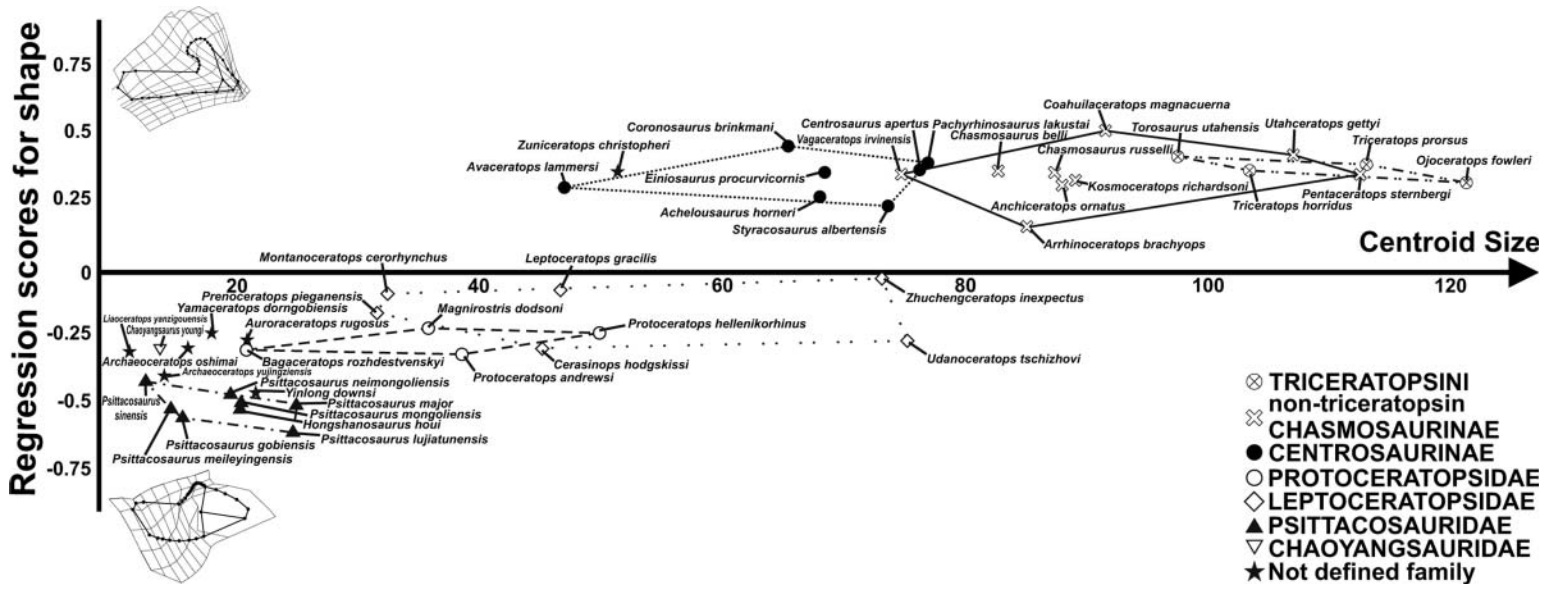

Fig. 7. Relationship between lower jaw morphology and size. The continuous line represents non-triceratopsin Chasmosaurinae morphospace. The dotted line represents Centrosaurinae morphospace. The double dot-dashed line represents Triceratopsini morphospace. The dashed line represents Protoceratopsidae morphospace. The double dotted line represents Leptoceratopsidae morphospace and the dot-dashed line represents Psittacosauridae morphospace.

Linear models and comparative methods

When evaluating phenotypic differences, the results highlight significant differences in shape and size among clades (Tables 2 and 3). The pair-wise perMANOVAs performed on shape variables revealed major clades with different cranial morphology, with the exception of Leptoceratopsidae, which has a similar cranial shape to Protoceratopsidae (Table 2), even when exploring the frill and the skull without frill shapes. When investigating the lower jaw shape, all groups possess distinct morphologies, with the exception of protoceratopsids, which share a similar lower jaw with leptoceratopsids, non-triceratopsin chasmosaurines relative to Centrosaurinae, and Triceratopsini, which has a different lower jaw compared with Centrosaurinae only (Table 2).

Table 2. Pair-wise perMANOVA performed on the shape variables by group in the four datasets

	Tricer	N-t Chasmo	Centro	Proto	Lepto	Psittaco
Skulls						
Triceratopsini	—	**0.0016**	**0.0002**	**0.011**	**0.0001**	**0.0001**
N-t Chasmosaurinae		—	**0.001**	**0.0001**	**0.0001**	**0.0001**
Centrosaurinae			—	**0.005**	**0.017**	**0.0001**
Protoceratopsidae				—	0.2	**0.006**
Leptoceratopsidae					—	**0.0001**
Psittacosauridae						—
Skulls without frill						
Triceratopsini	—	**0.006**	**0.0001**	**0.0001**	**0.0001**	**0.0001**
N-t Chasmosaurinae		—	**0.0001**	**0.0001**	**0.0001**	**0.0002**
Centrosaurinae			—	**0.0001**	**0.005**	**0.0001**
Protoceratopsidae				—	0.914	**0.0001**
Leptoceratopsidae					—	**0.0001**
Psittacosauridae						—
Frills						
Triceratopsini	—	**0.0019**	**0.0001**	**0.010**	**0.014**	**0.0006**
N-t Chasmosaurinae		—	**0.0001**	**0.0001**	**0.0001**	**0.0001**
Centrosaurinae			—	**0.005**	**0.004**	**0.0001**
Protoceratopsidae				—	0.1	**0.006**
Leptoceratopsidae					—	**0.0001**
Psittacosauridae						—
Lower jaws						
Triceratopsini	—	0.062	**0.001**	**0.0001**	**0.0001**	**0.0004**
N-t Chasmosaurinae		—	0.057	**0.0001**	**0.0001**	**0.0001**
Centrosaurinae			—	**0.004**	**0.0001**	**0.0001**
Protoceratopsidae				—	0.22	**0.0001**
Leptoceratopsidae					—	**0.0001**
Psittacosauridae						—

Note: Statistically significant results ($P < 0.05$) are indicated in **bold**. Tricer = Triceratopsini, N-t Chasmo = Non-triceratopsin Chasmosaurinae, Centro = Centrosaurinae, Proto = Protoceratopsidae, Lepto = Leptoceratopsidae, Psittaco = Psittacosauridae.

Pair-wise perANOVAs show clear differences in size among the major clades. Triceratopsins are significantly larger than non-triceratopsin ceratopsids in terms of the snout and lower jaw only. Non-triceratopsin chasmosaurines and centrosaurines have similar sizes, with the exception of the frill and lower jaw (Table 3 and Fig. S9). When exploring size differences of the lower jaw, Leptoceratopsidae is not significantly different from Centrosaurinae and Protoceratopsidae. In general, leptoceratopsids are as large as protoceratopsids (Table 3).

The results of OLS regression between cranial or frill shape and the percentage of angiosperm occurrences during the Cretaceous period highlight significant relationships (skulls: $R^2 = 0.342$, $P = 0.001$; frills: $R^2 = 0.398$, $P = 0.001$). At high percentages of angiosperm occurrence the skull is chasmosaurine-like, while at low percentages it is psittacosaurid-like (Fig. 8).

Table 3. Pair-wise perANOVA performed on the size variable by group in the four datasets

	Tricer	N-t Chasmo	Centro	Proto	Lepto	Psittaco
Skulls						
Triceratopsini	—	0.11	**0.003**	**0.011**	**0.034**	**0.0006**
N-t Chasmosaurinae		—	0.078	**0.004**	**0.0001**	**0.0001**
Centrosaurinae			—	**0.004**	**0.016**	**0.0001**
Protoceratopsidae				—	0.9	**0.011**
Leptoceratopsidae					—	**0.023**
Psittacosauridae						—
Skulls without frill						
Triceratopsini	—	**0.028**	**0.034**	**0.0001**	**0.0001**	**0.0001**
N-t Chasmosaurinae		—	0.81	**0.0001**	**0.0001**	**0.0001**
Centrosaurinae			—	**0.0001**	**0.006**	**0.0001**
Protoceratopsidae				—	0.54	**0.005**
Leptoceratopsidae					—	**0.0001**
Psittacosauridae						—
Frills						
Triceratopsini	—	0.32	**0.0008**	**0.0001**	**0.0001**	**0.0006**
N-t Chasmosaurinae		—	**0.005**	**0.0032**	**0.0001**	**0.0001**
Centrosaurinae			—	**0.0001**	**0.005**	**0.0003**
Protoceratopsidae				—	0.4	**0.0057**
Leptoceratopsidae					—	**0.0059**
Psittacosauridae						—
Lower jaws						
Triceratopsini	—	**0.022**	**0.004**	**0.0001**	**0.0092**	**0.0001**
N-t Chasmosaurinae		—	**0.0001**	**0.0001**	**0.0002**	**0.0001**
Centrosaurinae			—	**0.006**	0.062	**0.0002**
Protoceratopsidae				—	0.2	**0.0064**
Leptoceratopsidae					—	**0.0008**
Psittacosauridae						—

Note: Statistically significant results ($P < 0.05$) are indicated in **bold**. Tricer = Triceratopsini, N-t Chasmo = Non-triceratopsin Chasmosaurinae, Centro = Centrosaurinae, Proto = Protoceratopsidae, Lepto = Leptoceratopsidae, Psittaco = Psittacosauridae.

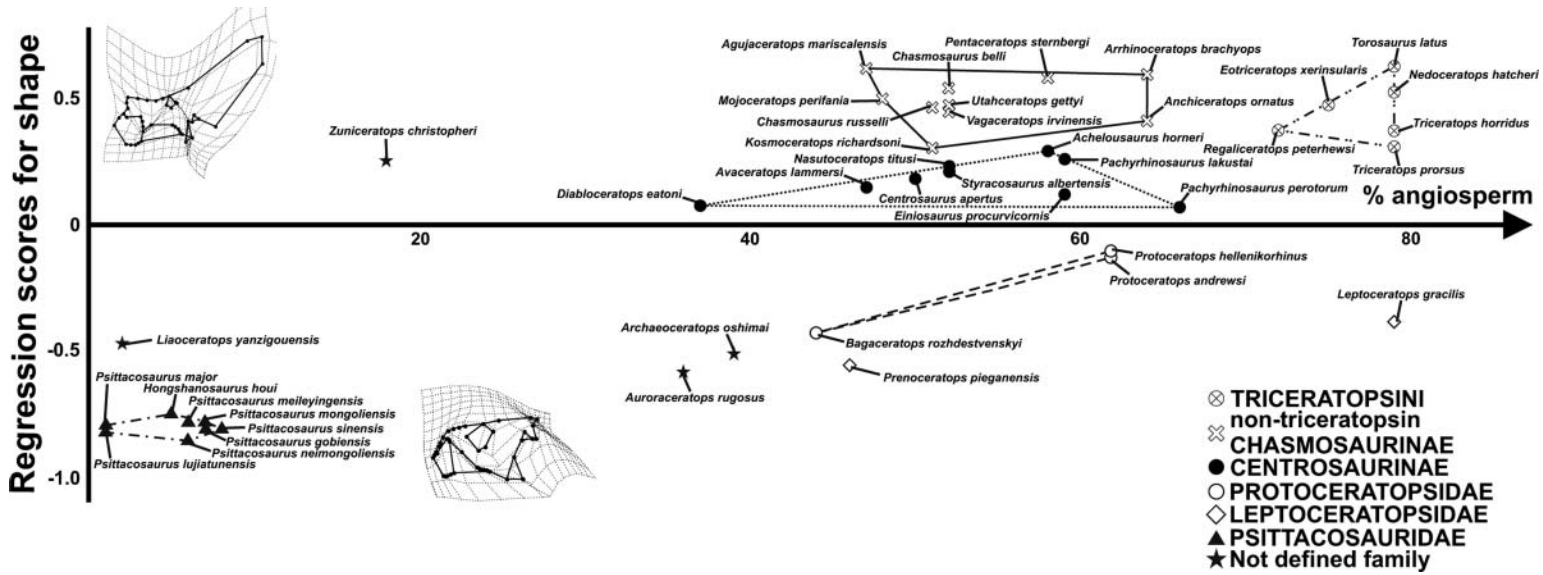

Fig. 8. Relationship between skull shape and angiosperm occurrence (expressed in percentages). The continuous line represents non-triceratopsin Chasmosaurinae morphospace. The dotted line represents Centrosaurinae morphospace. The double dot-dashed line represents Triceratopsini morphospace. The dashed line represents Protoceratopsidae morphospace and the dot-dashed line represents Psittacosauridae morphospace.

Shape is phylogenetically structured in the four datasets (skulls, skulls without frill, frills, and lower jaws) as revealed by the results of the physignal( ) function ($P = 0.001$). When accounting for phylogeny within the four datasets, using the phylosig( ) function, we found that size (CS) was phylogenetically structured as well ($P = 0.001$).

Morphological integration

Results of morphological integration (rarefied RV coefficient) between skulls (entire skull, skull without frill, and the frill alone) and lower jaws for the pooled sample and for the five clades (Centrosaurinae, non-triceratopsin Chasmosaurinae, Protoceratopsidae, Leptoceratopsidae, and Psittacosauridae) are shown in Table 4. Only the pooled comparisons are statistically supported with the exception of the clade Psittacosauridae, which appears to have a skull without frill highly integrated with the lower jaw, and centrosaurines, which have a frill highly integrated with the lower jaw (Table 4). The frill is much more integrated with the lower jaw than the skull with the frill excluded within Ceratopsia. When integrating the frill and the skull without frill, Triceratopsini is more integrated than non-triceratopsin chasmosaurines (Table 5).

Table 4. RV coefficients and the associated simulated *P*-values after 1000 permutations for testing co-variation between skulls (three configurations) and lower jaws within Ceratopsia (pooled sample) and within the clades under investigation

Clade	RV	*P*-value
Skulls		
Pooled sample	**0.86053**	**0.0001**
Chasmosaurinae	0.813236	0.7659
Centrosaurinae	0.813007	0.58241
Protoceratopsidae	0.71232	0.6733
Psittacosauridae	0.87509	0.099
Skulls without frill		
Pooled sample	**0.76128**	**0.0001**
Chasmosaurinae	0.84081	0.3471
Centrosaurinae	0.82918	0.5374
Protoceratopsidae	0.96802	0.1778
Leptoceratopsidae	0.84719	0.32867
Psittacosauridae	**0.89591**	**0.0312**
Frills		
Pooled sample	**0.8113**	**0.0001**
Chasmosaurinae	0.77186	0.0742
Centrosaurinae	**0.92676**	**0.016**
Protoceratopsidae	0.7447	0.6713
Leptoceratopsidae	0.46115	0.98
Psittacosauridae	0.76475	0.8521

Note: Significant results are shown in **bold**.

Table 5. RV coefficients and the associated simulated *P*-values after 1000 permutations for testing co-variation between skulls with the frill excluded and frills alone within Ceratopsia (pooled sample) and within the clades under investigation

Clade	RV	*P*-value
Pooled sample	**0.80611**	**0.0001**
Triceratopsini	**0.92898**	**0.028**
N-t Chasmosaurinae	**0.88771**	**0.004**
Centrosaurinae	0.85856	0.074
Protoceratopsidae	0.91215	0.3196
Psittacosauridae	0.84077	0.1838

Note: Significant results are shown in **bold**. N-t Chasmosaurinae = Non-triceratopsin Chasmosaurinae.

Morphological integration results and *P*-values (rarefied RV coefficient), using a part–whole approach, between the entire skull, skull without frill, and the frill alone for the pooled samples and for the five clades are shown in Table S6. The frill and the skull without frill of Triceratopsini appear to be highly integrated with the entire skull within Ceratopsidae. Psittacosaurids have a skull without frill more integrated with the entire skull relative to other ceratopsian clades (Table S6). In general, the frill is much more integrated with the overall cranial shape than the skull without the frill within Ceratopsia.

Figure 9 shows the morphological covariation between the skull in lateral view and the lower jaw, based on the partial least square analysis (PLS) performed on the pooled dataset. The first pair of singular axes (SAs) explains 67.063% of the overall covariance. At negative SA1 values the skull is psittacosaurid-like, having a short and deep snout, no nasal horn, short premaxilla, large orbit, and an incipient frill, all of which are associated with the lower jaw having a short and massive dentary, short coronoid process, and caudally elongated angular and surangular. Positive SA1 values correspond to a ceratopsid-like skull, bearing a dorsally pronounced nasal horn, longer and deep snout, small orbit, and a frill dorso-caudally expanded, which is associated with the lower jaw having a long and slender dentary, a dorsally developed hooked coronoid process, and a short angular and surangular.

The morphological covariation of the skulls without the frill and the frills alone are shown in Fig. 10. The first pair of singular axes (SAs) explains 65.089% of the overall covariance. Negative SA1 values are associated with a psittacosaurid-like skull without the frill, having a short and deep snout, no nasal horn, a short premaxilla, and an incipient parieto-squamosal complex, with a large infratemporal fenestra and rostral tip of the supratemporal fenestra located forward of the infratemporal fenestra, whereas at positive SA1 values the skull without a frill is ceratopsid-like, with a developed nasal horn, longer premaxilla-maxilla, and ventral tip of the quadrate located slightly behind the jugal tip, associated with a chasmosaurine-like and caudo-dorsally expanded frill. It bears an elongated and triangular squamosal, a small infratemporal fenestra, and a rostral tip of the supratemporal fenestra located well forward of the infratemporal fenestra.

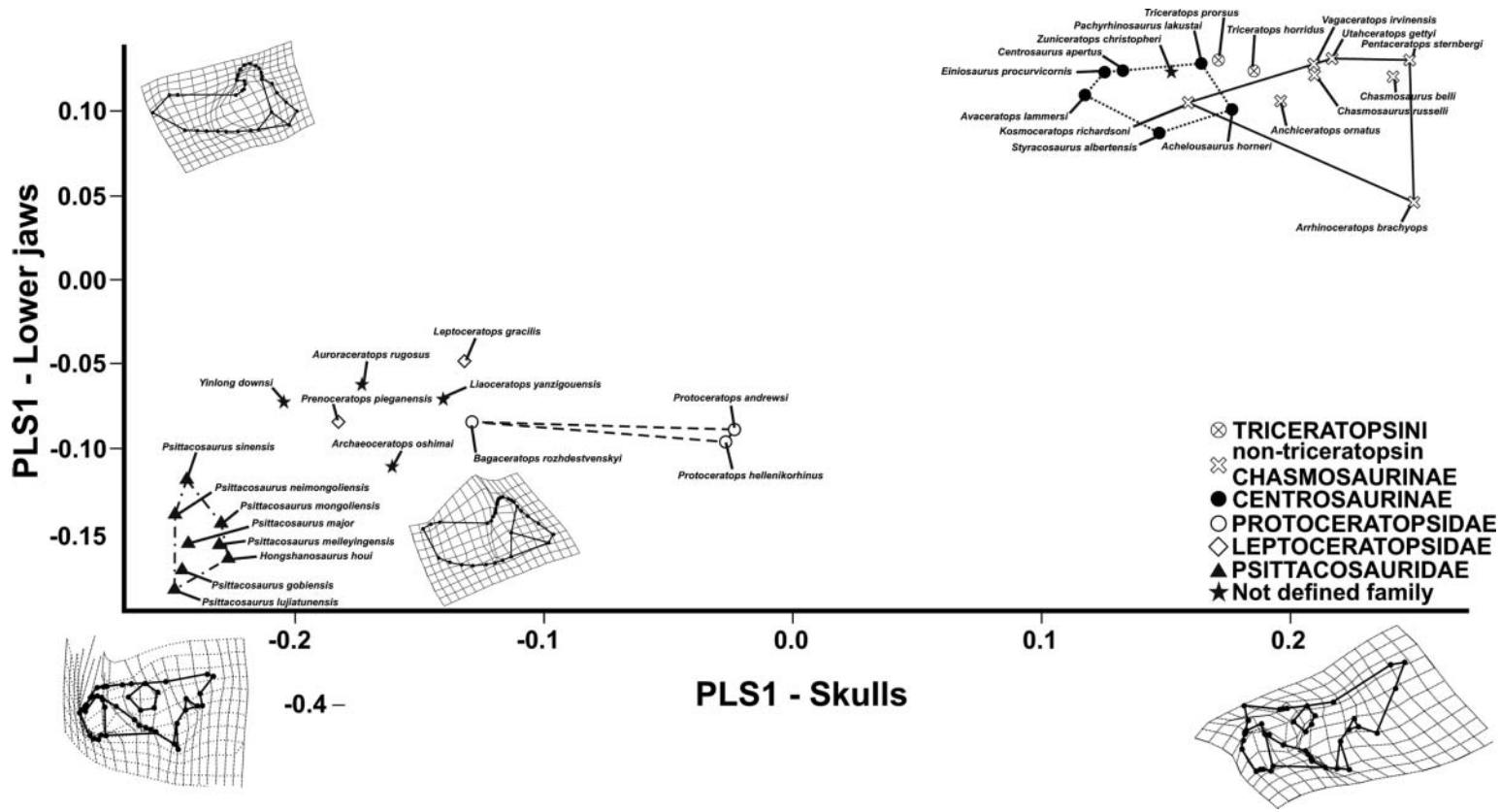

Fig. 9. Morphological covariation between skulls and lower jaws. The continuous line represents non-triceratopsin Chasmosaurinae morphospace. The dotted line represents Centrosaurinae morphospace. The dashed line represents Protoceratopsidae morphospace and the dot-dashed line represents Psittacosauridae morphospace.

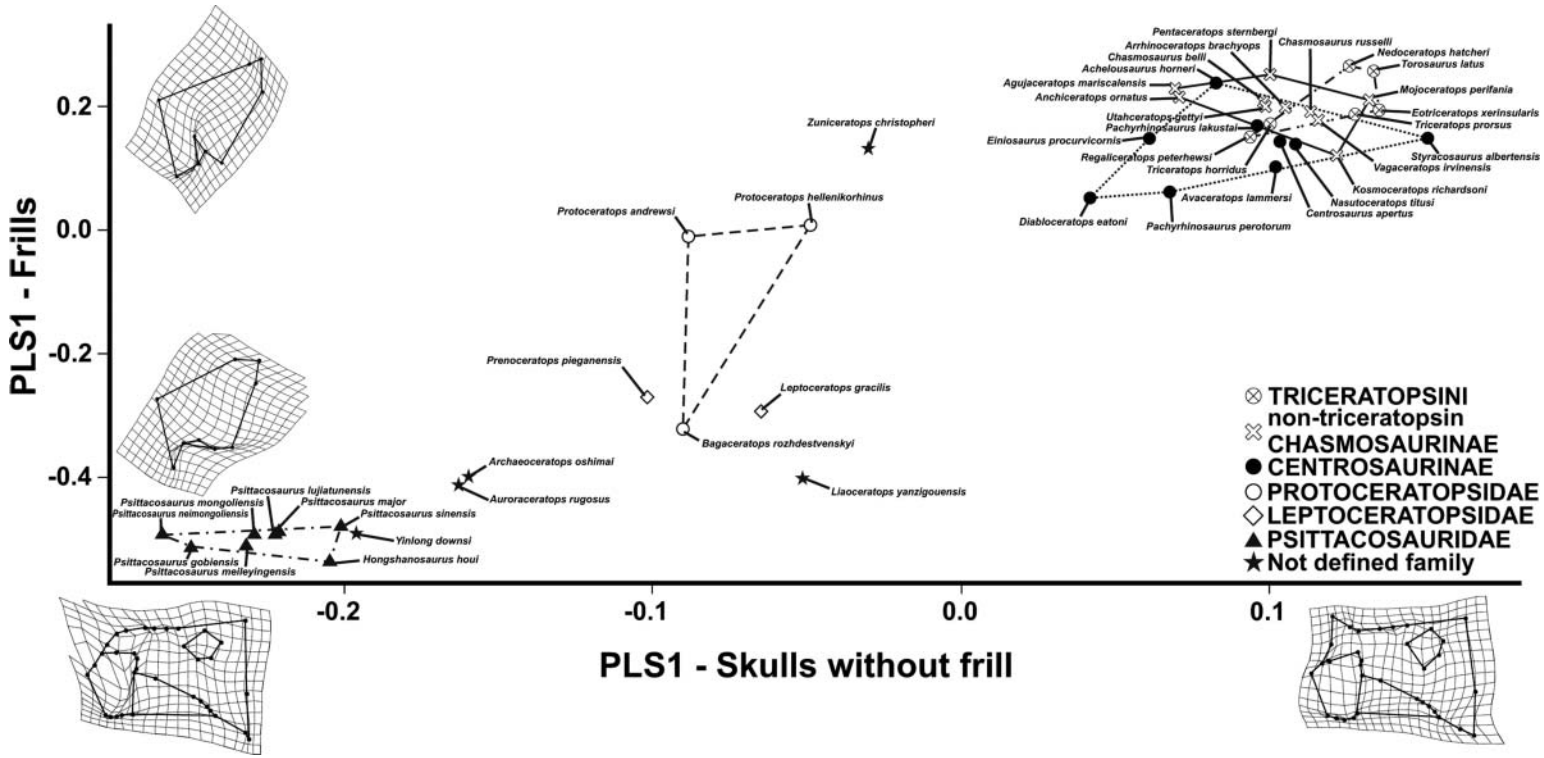

Fig. 10. Morphological covariation between skulls without frill and frills alone. The continuous line represents non-triceratopsin Chasmosaurinae morphospace. The dotted line represents Centrosaurinae morphospace. The dashed line represents Protoceratopsidae morphospace and the dot-dashed line represents Psittacosauridae morphospace.

For the shape covariation of the skulls without frill and the frills alone associated with the lower jaws, see text and Figs. S11 and S12 in 3008Appendix.

Phenotypic evolutionary rates

Investigating evolutionary shifts of multivariate data (shape) within the ceratopsian phylogeny permits a better evaluation of the tempo and mode of evolution in the history of this clade. The transformPhylo.ML( ) and traitMedusaSummary( ) functions of the 'MOTMOT' R package allow the identification and visualization of internal nodes where a particular shift occurs on the phylogenetic tree (see Fig. 3). In this analysis, we considered only ceratopsian species represented by a complete or an almost complete skull or lower jaw.

Regarding the overall cranial shape within Ceratopsia, a negative phenotypic shift occurs at the node that corresponds with the morphologically basal clade Psittacosauridae, whereas a positive shift occurs at the base of the morphologically derived clade Ceratopsidae (Fig. 11A). The phenotypic rate analysis performed on shape of the lower jaw highlights a negative evolutionary shift at the clade Psittacosauridae corresponding to a slowdown of the rate, whereas an evolutionary shift is identified at the basal node of Triceratopsini corresponding to an acceleration in rate (Fig. 11B). Branch lengths are short when there is a slowdown of phenotypic evolutionary rate and longer when an accelerated rate is identified in a particular node of the phylogeny.

Details of phenotypic evolutionary shifts for skulls without frill and the frills alone are shown in Fig. S13, while pair-wise comparisons between groups are reported in 3008Appendix and Table S7.

When comparing the different evolutionary rates on shape among clades, the results reveal that Centrosaurinae has the fastest evolutionary rate for cranial shape within Ceratopsia, whereas Chasmosaurinae exhibits the fastest rate on shape in the lower jaw dataset. By contrast, Psittacosauridae has the slowest evolutionary rate on shape with the exception of the frill (Table 6).

In general, Ceratopsia exhibits an overall slowdown of the phenotypic evolutionary rate early in its evolutionary history (Early Cretaceous). In the Late Cretaceous, an acceleration of phenotypic rates mainly characterizes Ceratopsoidea in relation to cranial shape (skull and skull without frill). By contrast, a slowdown of the rate during the Early Cretaceous characterizes the basal ceratopsian members in relation to the lower jaw shape. Ceratopsidae shows the fastest rates when compared with other clades (Table 6). However, a progressive increase in the evolutionary rate is observed from the basal to the more derived clades (Table 6).

DISCUSSION

Investigating changes in cranial and lower jaw shape among the several ceratopsian clades and species provides a better understanding of the evolution of the group through time. Our work suggests that the frill primarily evolved to better co-vary with the lower jaw to produce an efficient masticatory apparatus, while also driving overall cranial shape through time. Secondarily, the changes in frill shape are correlated with the angiosperm diversification that occurred during the Cretaceous period. The evolution of the frill within Ceratopsia thus seems to be correlated with changes in diet.

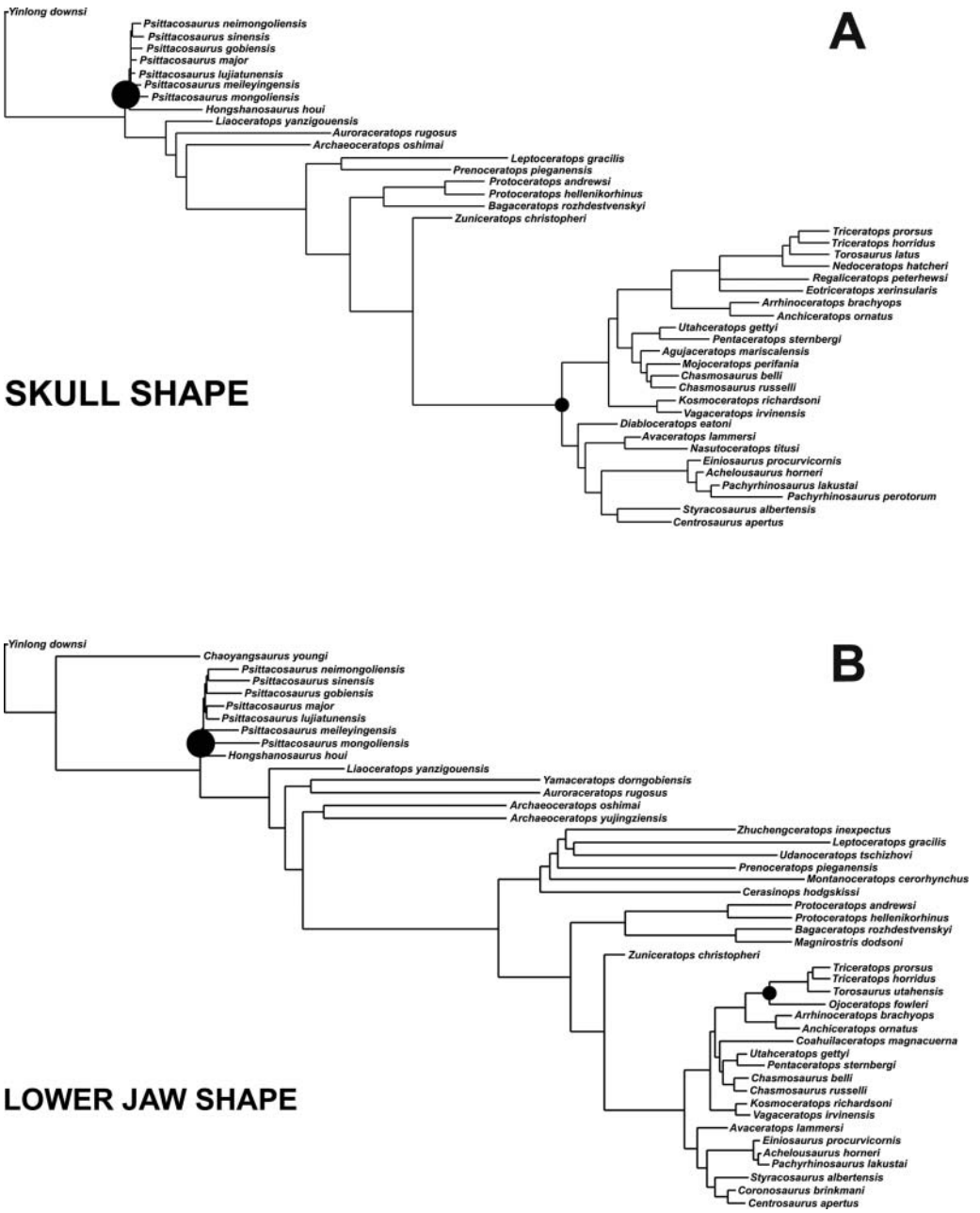

Fig. 11. Phylogenetic tree with branch lengths proportional to phenotypic evolutionary rates for skull shape (A) and lower jaw shape (B). Solid dots identify the main phenotypic shifts along the phylogeny. Large dot indicates the major shift, whereas the small one indicates the minor shift.

Table 6. Evolutionary rates for shape within each clade in the four datasets

Clade	Skulls	Skulls without frill	Frills	Lower jaws
Chasmosaurinae	1.4180	1.385	1.052	2.277
Centrosaurinae	3.3113	2.807	1.717	1.129
Protoceratopsidae	0.8098	1.043	0.294	1.151
Leptoceratopsidae	0.6811	0.481	1.609	0.930
Psittacosauridae	0.2720	0.298	1.154	0.178

When looking at shape differences among ceratopsians, the results of PCAs and permANOVAs highlight distinct shapes for each clade when investigating the various cranial and lower jaw morphologies. *Yinlong downsi*, the most basal known member of Ceratopsia, shows a nearly unique and primitive morphology, particularly for the lower jaw. The whole skull is similar to those of other basal taxa such as *Archaeoceratops*, *Liaoceratops*, and *Auroraceratops* (Xu *et al.*, 2006), but when considering the facial portion alone, the skull appears different from those of all other ceratopsians (Figs. S5B and S6). By contrast, the frill alone in lateral view resembles the psittacosaurid morphology.

Psittacosauridae is found to be a basal clade that is rather conservative in shape. It has a cranial and lower jaw morphology distinct from that seen in other ceratopsian taxa. All psittacosaurid species lie close to each other, suggesting a very similar cranial and lower jaw shape. This is consistent with previous suggestions that the members of this clade, due to their body size (1–2 m in body length), conservative cranial morphology, and limited spatiotemporal range (10–20 million years), were dietary specialists (Sereno *et al.*, 2010). Nevertheless, *Hongshanosaurus houi* appears to be morphologically different from other psittacosaurids when looking at the overall cranial shape (Fig. 4) and the snout in particular (Fig. S5B). Those findings seem to support the hypothesis that *Hongshanosaurus* pertains to a distinct and valid genus (see You and Xu, 2005). By contrast, recent morphometric and systematic assessments (Sereno, 2010; Hedrick and Dodson, 2013) have suggested that *Hongshanosaurus* should be considered as a junior synonym of *Psittacosaurus lujiatunensis* of the Lujiatun beds of the Yixian Formation (Barremian in age), China, with apparent differences due to taphonomy.

The skulls of *Leptoceratops* and *Prenoceratops* resemble the morphologies of basal neoceratopsians such as *Archaeoceratops*, *Auroraceratops*, *Liaoceratops*, and those of protoceratopsids (Fig. 4 and Table 2). Leptoceratopsids represent a clade with wide morphological variation within the lower jaw. Morphology within members of this clade resembles that of the lower jaw of Protoceratopsidae, as well as those of basal neoceratopsians, such as *Archaeoceratops*, *Liaoceratops*, and *Yamaceratops* (Fig. 5). Combinations of several anatomical features such as a short parieto-squamosal frill, a massive lower jaw, and relatively massive teeth may reflect adaptations to different environments and food resources (Xu *et al.*, 2010a).

Protoceratopsids show an intermediate morphology between the most derived clade Ceratopsidae and basal neoceratopsians in terms of shape changes of the whole skull and the frill alone. For shape variation of the skull without the frill, Protoceratopsidae resembles the primitive condition of leptoceratopsids and basal taxa (Figs. S5 and S6). The frill has two different shape 'trajectories', whereby *Protoceratops* spp. resemble the ceratopsid condition, while *Bagaceratops* is closer to the shape seen in basal neoceratopsians (Fig. S7). Protoceratopsids have a moderately broad lower jaw shape variation. The lower jaw in

Protoceratops hellenikorhinus resembles the lower jaw of leptoceratopsids, whereas the other protoceratopsids possess a lower jaw similar to that of basal neoceratopsians (Figs. 5 and Fig. S4).

Zuniceratops christopheri, sister taxon of Ceratopsidae, has an overall cranial shape intermediate between that of Centrosaurinae and Chasmosaurinae. For the facial portion of the skull, *Zuniceratops* shows an intermediate shape between Ceratopsidae and Protoceratopsidae. It possesses a combination of primitive and derived characters (You and Dodson, 2004). After all, it shares with some protoceratopsids (*Magnirostris* and *Bagaceratops*), and with a derived taxon (*Diabloceratops eatoni*), plesiomorphic traits such as an accessory antorbital fenestra (Kirkland and DeBlieux, 2010). However, the skull of *Zuniceratops* is heavily reconstructed, the frill in particular. All of these systematic considerations need further and better fossil material to assess the morphological aspects of this taxon and its relationship with other ceratopsian taxa.

Ceratopsidae represents the most speciose clade within Ceratopsia (Dodson *et al.*, 2004; Sampson *et al.*, 2010, 2013) and is well represented in this study. Non-triceratopsin Chasmosaurinae is well separated from Centrosaurinae and Triceratopsini in terms of cranial variation (entire skulls, skulls without frill, and frills alone; see also Table 2). Triceratopsins (derived chasmosaurines) have a distinct cranial shape compared with non-triceratopsin chasmosaurines, for the frill in particular (Fig. 4 and Fig. S7). Centrosaurinae has a different cranial shape from Chasmosaurinae, for the entire skull, skull without the frill, and frill shape alone. Basal centrosaurines – *Diabloceratops*, *Avaceratops*, and *Nasutoceratops* – are different from derived centrosaurines in cranial shape (Fig. 4 and Figs. S3, S5, and S6), while derived centrosaurines possess a similar cranial morphology.

Triceratopsins have significantly different lower jaw morphology than Centrosaurinae, whereas they share a similar shape with non-triceratopsin Chasmosaurinae. Recent contributions highlighted the different morphology of Triceratopsini compared with other ceratopsids (Mallon *et al.*, 2014; Maiorino *et al.*, 2015b), for the coronoid process in particular. The different findings reported above are probably associated with the different landmark configuration selected compared with that used by Maiorino and colleagues (2015b). In fact, the pair-wise perMANOVA *P*-values (Table 2) are close to 0.05, the limit of statistical significance selected here, suggesting no clear lower jaw shape difference between Triceratopsini and non-triceratopsin chasmosaurines.

No evolutionary allometry is observed within Ceratopsia or within any clade (Table 1). The shape variation of the ceratopsian skull is independent of the size increase through time.

Exploring the morphological integration between the skull and lower jaw, and between the frill and the rest of the skull without the frill, allows us to assess which clade has the overall cranial configuration that best fits with that of the lower jaw, and which clade has the cranial configuration with the frill excluded that best fits with that of the frill. Overall, this exercise allows us to evaluate the 'best' morphological arrangement of the feeding apparatus within Ceratopsia (see Tables 4 and 5 and Table S6). The rarefied RV coefficient has been used to quantify the covariation between subsets of landmarks. Morphological integration predicts that strongly co-varying modules will co-evolve because of their contemporaneous response to selection. Functional integration is expected to occur when the modules share a common function (Cheverud, 1996; Piras *et al.*, 2010).

We found that frill shape, rather than the facial portion of the skull, is the main driving force in overall skull shape within Ceratopsia, and within Triceratopsini in particular (see Table S6). The elongation of the frill, as seen in Ceratopsidae, seems to be strongly

correlated with the elongation of the coronoid process, the lowering of the joint in the lower jaw, and the consequent backward tilt of the muscle action line (Ostrom, 1966; Mallon and Anderson, 2015). As argued in Ostrom (1966) and Dodson (1993, 1996), the elongation of the frill and the reduction of the infratemporal fenestra led to a reduction in size of the adductor chamber and the occupation of the adductor muscles at the base of the frill. These modifications were accompanied by forward rotation of the ventral end of the quadrate with an enlargement and backward shift of the jugal (Dodson, 1993; Dodson *et al.*, 2004) to improve the feeding apparatus in derived ceratopsians.

Our results suggest that the frill evolved primarily and initially as a mechanical response to several selective pressures for a tighter covariation with the lower jaw morphology and to permit better performance for the masticatory apparatus. In particular, we find a correlation between cranial and frill shape with the percentage of angiosperms in the Cretaceous palaeoenvironments (Fig. 8). The frill perhaps evolved in response to changing dietary function associated with the turnover between gymnosperms and angiosperms in the Cretaceous (Stanley, 2009), within Ceratopsidae in particular, together with probable competition with other groups of coeval megaherbivorous dinosaurs (e.g. hadrosaurids).

In contrast, other recent studies did not find a significant relationship between the co-evolution of angiosperms (major radiations occurred during the Albian–Cenomanian and Santonian–Maastrichtian stages) and faunal changes of herbivorous dinosaurs during the Cretaceous, particularly for Ceratopsia (Weishampel and Jianu, 2000; Barrett and Willis, 2001; Butler *et al.*, 2009), even if this hypothesis has still been invoked in recent works (Tiffney, 2004; Coria and Salgado, 2005). The differences with our study may be because we examined morphology itself, rather than species counts. We suggest that additional morphological studies would be useful, in addition to species diversity counts. Moreover, the origins of the clade Leptoceratopsidae (during the Albian–Cenomanian stages) and the clade Ceratopsidae (at the base of the Campanian stage, or alternatively during the Santonian; see Fig. 3) highlight a potential relationship between angiosperm diversification and the ceratopsian radiation during the Cretaceous. Nevertheless, those results should be considered preliminary and further investigations are required on the issue.

Sexual selection or species recognition may also have driven the morphological variation of extra ornamentations and not the frill itself. Indeed, the mechanical response may have driven the shape changes of the frill through time. This includes an enlargement of the frill to provide a better framework for the adductor muscle [located in the anterior-most part (Dodson, 1996)] and a further elongation, with the development of epi-ossifications, under sexual selection/species recognition pressure. Makovicky and Norell (2006) highlighted the frill as a potential exaptation, primarily as a framework for the jaw muscle attachments (in basal neoceratopsians) and secondarily as a display structure (within Ceratopsidae). Our findings are consistent with this hypothesis.

Recent contributions have hypothesized that distinct cranial morphologies within the two ceratopsid subfamilies probably evolved as an ecological response to niche partitioning (Henderson, 2010; Mallon and Anderson, 2013, 2014). Those cranial differences were related to a mechanical response to make a more resistant structure, facilitating niche partitioning with different diets. The rarefied RV values reported here partially support this hypothesis (see Table 5 and Table S7). The centrosaurine facial portion of the cranium is less integrated with the frill compared with non-triceratopsin Chasmosaurinae and Triceratopsini (the latter registering the highest value), and the centrosaurine frill is less integrated with the overall cranial configuration compared with the other ceratopsids. Additionally, centro-

saurines possess a frill that is well integrated with the lower jaw (RV = 0.926) compared with other ceratopsids. These results support the idea of the evolution of the snout and the frill as a mechanical response to distinct ecological niches and food resources within Ceratopsidae. In addition, a frill much better integrated with the overall skull and with the facial portion in Triceratopsini, relative to other ceratopsids, would have evolved to compensate a stressed lower jaw, as shown by Maiorino and colleagues (2015b).

The basal clade Psittacosauridae represents a clade where the facial portion of the skull is well integrated with the lower jaw. The absence of a tall and wide frill, a short snout, and laterally expanded jugals represent a combination of characters that strongly co-vary with the lower jaw. We found no significant integration between the psittacosaurid frill and lower jaw, whereas the facial portion is better integrated (see Table 4). As argued by Sereno and colleagues (2010), the psittacosaurid cranium represents a structure that was able to tolerate the large bite forces generated by enlarged jaw muscles. The short snout, with an elevated and small external nares and the absence of antorbital fenestra, could increase the bite force at the beak margin. Psittacosaurids potentially evolved a short snout and wide cheekbones (Makovicky, 2012) as a mechanical response to compensate for the non-integration of the frill with the lower jaw. The lower jaw is short with a moderately sized coronoid process, short and broad predentary, and a long and slender angular and surangular (You and Dodson, 2004; Tanoue *et al.*, 2010). These modifications produced a facial portion of the cranium that was well integrated with the lower jaw, and we think it is a reasonable explanation for their conservative size and shape.

Exploring the evolutionary rates of shape change on the phylogeny allows us to infer where the phenotypic rate change became slow or fast and which node represents an important shift for those variables. Derived clades (centrosaurines and chasmosaurines) show an increasing rate through time relative to the basal clades in the four datasets (Table 6 and Table S7). The evolutionary rates within Ceratopsia are not constant through time, but they are slow in the early history of the clade and then become faster, during the mid-Late Cretaceous. These results appear to be related to previous results concerning disparity, morphological integration, and phylogenetic signal reported above. The co-evolution of the frill and snout within Ceratopsidae is characterized by an increasing evolutionary rate. Basal taxa, including Psittacosauridae and Leptoceratopsidae, show a decreasing rate in the evolution of shape as expected in the light of the results reported above, in particular regarding the conservative shape and size of the clade Psittacosauridae. This latter clade shows the most integrated facial portion of the skull with the lower jaw among ceratopsians. The analyses confirm that the morphological variation of the skull increases during the mid-Late Cretaceous. This increase is mainly due to the development of the large frill in Coronosauria.

Those modifications (e.g. short and deep cranium) appear to be related to dietary niche partitioning within Ceratopsidae (Henderson, 2010; Mallon and Anderson, 2013, 2014). Visual display is also a reasonable secondary role of the parieto-squamosal complex. However, those modifications could also be related to the angiosperm expansion that occurred in the Cretaceous period. The radiation of leptoceratopsids and ceratopsids (Figs. 3 and 8) occurred when flowering plants diversified. This event could have affected the habitats where leptoceratopsids or ceratopsids lived. Maiorino *et al.* (2015b) noted that Triceratopsini possessed a lower jaw more subject to stress when chewing compared with other ceratopsids. They suggested that the different mechanical behaviours could be correlated with different diets. *Triceratops* and its closest relatives lived in environments dominated by angiosperms

rather than gymnosperms, which dominated the Campanian and Maastrichtian habitats (Lupia *et al.*, 2000; Braman and Koppelhus, 2005; Arens *et al.*, 2014; Arens and Allen, 2014). Based on our results, lower jaws show an increase of phenotypic evolutionary rate at the base of Triceratopsini. This finding is in line with Maiorino *et al.* (2015b) in that triceratopsins possess a distinct lower jaw shape relative to non-triceratopsin ceratopsids (particularly centrosaurines).

The Campanian stage would appear to be a critical time span for the diversity and evolution of Ceratopsia when exploring the morphological variation of skulls and lower jaws. At this time, the cranial morphology and frill ornamentation within Ceratopsia show the greatest disparity, while the lower jaw shows the least. New fossil discoveries and new research in fields related to palaeontology could provide new insights on this time interval and show how ceratopsians achieved this incredible cranial disparity.

Finally, we discuss an issue with the dataset. Although we researched the most comprehensive sample of skulls and lower jaws of Ceratopsia, the leptoceratopsids (there are two nearly complete skulls in the sample, one of *Leptoceratops* and one of *Prenoceratops*) and protoceratopsids are not well represented by complete skulls (most of the protoceratopsid material is represented by *Protoceratops andrewsi*). The sample size of these two clades may have had an effect on the results, even if this is what is known in the fossil record. New fossil material is needed to confirm the results reported above. However, we are confident that the results reported here are reasonable for reconstructing broad patterns when considering the wide morphological variation of the skulls and lower jaws analysed here.

CONCLUSIONS

The evolutionary history of Ceratopsia is strongly affected by phylogeny for both shape and size. The evolution of the frill within Ceratopsia drives the morphological changes of the entire skull. Evolving a dorso-caudally expanded frill necessarily requires elongation and depression of the facial portion of the cranium and a dorsally elongated coronoid process for a better covariation between skull and lower jaw, and therefore for a more efficient feeding apparatus as seen in ceratopsids. Morphological integration and evolutionary rate analyses highlight a change in the evolutionary history of ceratopsians after the origin of the coronosaurs, as well as within the more restricted clade of Ceratopsoidea, along with an increase in morphological variation (mainly in skull shape) during the mid-Late Cretaceous (Santonian–Campanian).

In the early history of Ceratopsia (e.g. Psittacosauridae), cranial structures are well integrated with the lower jaw. During the evolution of the clade, as stated above, the diversification of angiosperms that occurred towards the end of the Early Cretaceous and end of the Late Cretaceous appear to have potentially affected the cranial and lower jaw modifications of ceratopsians, and the frill in particular. The development and elongation of the frill could be interpreted as a morphological response to the change in dietary composition (different fodder toughness).

The analyses reported here should be expanded upon, and we suggest this as a fruitful area for future exploration. New data on change in floral compositions could better test the hypotheses discussed above. Finally, new cranial material will provide morphological information and help in the investigation of the evolutionary history of Ceratopsia.

ACKNOWLEDGEMENTS

No conflict of interest exists among the authors of this work. We are grateful to many institution curators and their staff for allowing access to the collections in their care. Thanks to Peter L. Larson who provided useful suggestions. We also thank Dr. Gabriele Sansalone who collected some photographs of *Triceratops prorsus* at Bayerische Staatssammlung für Paläontologie und Historische Geologie, Munich, Germany, and for helpful suggestions and comments, as well as Dr. Anneke H. van Heteren who collected photographs of *Triceratops horridus* at Muséum National d'Histoire Naturelle, Paris, France.

REFERENCES

Adams, D.C. and Nistri, A. 2010. Ontogenetic convergence and evolution of foot morphology in European cave salamanders (Family: Plethodontidae). *BMC Evol. Biol.*, **10**: 1–10.

Adams, D.C. and Otarola-Castillo, E. 2013. Geomorph: an R package for the collection and analysis of geometric morphometric shape data. *Meth. Ecol. Evol.*, **4**: 393–399.

Adams, D.C., Rohlf, F.J. and Slice, D.E. 2004. Geometric morphometrics: ten years of progress following the 'revolution'. *Ital. J. Zool.*, **71**: 5–16.

Adams, D.C., Berns, C.M., Kozak, K.H. and Wiens, J.J. 2009. Are rates of species diversification correlated with rates of morphological evolution? *Proc. R. Soc. Lond. B: Biol. Sci.*, **276**: 2729–2738.

Arens, N.C. and Allen, S.E. 2014. A florule from the base of the Hell Creek Formation in the type area of eastern Montana: implications for vegetation and climate. In *Through the End of the Cretaceous in the Type Locality of the Hell Creek Formation in Montana and Adjacent Areas* (G.P. Wilson, W.A. Clemens, J.R. Horner and J.H. Hartman, eds.), pp. 173–208. Boulder, CO: Geological Society of America.

Arens, N.A., Thompson, A. and Jahren, A.H. 2014. A preliminary test of the press-pulse extinction hypothesis: palynological indicators of vegetation change preceding the Cretaceous–Paleogene boundary, McCone County, Montana, USA. In *Through the End of the Cretaceous in the Type Locality of the Hell Creek Formation in Montana and Adjacent Areas* (G.P. Wilson, W.A. Clemens, J.R. Horner and J.H. Hartman, eds.), pp. 209–228. Boulder, CO: Geological Society of America.

Arthur, M.A., Dean, W.E. and Schlanger, S.O. 1985. Variations in the global carbon cycle during the Cretaceous related to climate, volcanism, and changes in atmospheric CO_2. In *The Carbon Cycle and Atmospheric CO2: Natural Variations Archean to Present* (E.T. Sundquist and W.S. Broecker, eds.), pp. 504–529. AGU Monograph #32. Washington, DC: American Geophysical Union.

Atchley, W.R. and Hall, B.K. 1991. A model for development and evolution of complex morphological structures. *Biol. Rev. Camb. Phil.*, **66**: 101–157.

Atchley, W.R., Nordheim, E.V., Gunsett, F.C. and Crump, P.L. 1982. Geometric and probabilistic aspects of statistical distance functions. *Syst. Zool.*, **31**: 445–460.

Baab, K.L., McNulty, K.P. and Rohlf, F.J. 2012. The shape of human evolution: a geometric morphometrics perspective. *Evol. Anthropol.*, **21**: 151–165.

Badyaev, A.V. and Foresman, K.R. 2000. Extreme environmental change and evolution: stress-induced morphological variation is strongly concordant with patterns of evolutionary divergence in shrew mandibles. *Proc. R. Soc. Lond. B: Biol. Sci.*, **267**: 371–377.

Badyaev, A.V. and Foresman, K.R. 2004. Evolution of morphological integration. I. Functional units channel stress-induced variation in shrew mandibles. *Am. Nat.*, **163**: 868–879.

Badyaev, A.V., Foresman, K.R. and Young, R.L. 2005. Evolution of morphological integration. II. Developmental accommodation of stress-induced variation in shrew mandibles. *Am. Nat.*, **166**: 382–395.

Bakker, R.T. 1986. *The Dinosaur Heresies*. New York: William Morrow.

Barrett, P.M. and Rayfield, E.J. 2006. Ecological and evolutionary implications of dinosaur feeding behavior. *Trends Ecol. Evol.*, **21**: 217–224.

Barrett, P.M. and Willis, K.J. 2001. Did dinosaurs invent flowers? Dinosaur–angiosperm coevolution revisited. *Biol. Rev.*, **76**: 411–447.

Barron, E.J. 1983. A warm, equable Cretaceous – the nature of the problem. *Earth-Sci. Rev.*, **19**: 305–338.

Barron, E.J. 1985. Numerical climate modeling, a frontier in petroleum source rock prediction: results based on Cretaceous simulations. *AAPG Bull. Am. Assoc. Petrol. Geol.*, **69**: 448–459.

Berner, R.A., Lasaga, A.C. and Garrels, R.M. 1983. The carbonate-silicate geochemical cycle and its effect on atmospheric carbon dioxide over the past 100 million years. *Am. J. Sci.*, **283**: 641–683.

Bookstein, F.L. 1986. Size and shape spaces for landmark data in two dimensions. *Stat. Sci.*, **1**: 181–242.

Bookstein, F.L. 1991. *Morphometric Tools for Landmark Data: Geometry and Biology*. Cambridge: Cambridge University Press.

Bookstein, F.L. 2013. Allometry for the twenty-first century. *Biol. Theor.*, **7**: 10–25.

Bookstein, F.L., Schäfer, K., Prossinger, H., Seidler, H., Fieder, M., Weber, G.W. *et al.* 1999. Comparing frontal cranial profiles in archaic and modern *Homo* by morphometric analysis. *Anat. Rec.*, **257**: 217–224.

Bookstein, F.L., Streissguth, A.P., Sampson, P.D., Connor, P.D. and Barr, H.H. 2002. Corpus callosum shape and neuropsychological deficits in adult males with heavy fetal alcohol exposure. *NeuroImage*, **15**: 233–251.

Braman, D.R. and Koppelhus, E.B. 2005. Campanian Palynomorphs. In *Dinosaur Provincial Park, a Spectacular Ancient Ecosystem Revealed* (P.J. Currie and E.B. Koppelhus, eds.), pp. 101–130. Bloomington, IN: Indiana University Press.

Brown, B. and Schlaikjer, E.M. 1940. The structure and relationship of *Protoceratops*. *Ann. NY Acad. Sci.*, **40**: 133–265.

Brown, C.M. and Henderson, D.M. 2015. A new horned dinosaur reveals convergent evolution in cranial ornamentation in Ceratopsidae. *Curr. Biol.*, **25**: 1–8.

Brusatte, S.L., Nesbitt, S.J., Irmis, R.B., Butler, R.J., Benton, M.J. and Norell, M.A. 2010. The origin and early radiation of dinosaurs. *Earth-Sci. Rev.*, **101**: 68–100.

Brusatte, S.L., Sakamoto, M., Montanari, S. and Harcourt Smith, W.E.H. 2011. The evolution of cranial form and function in theropod dinosaurs: insights from geometric morphometrics. *J. Evol. Biol.*, **25**: 365–377.

Butler, R.J., Barrett, P.M., Kenrick, P. and Penn, M.G. 2009. Testing co-evolutionary hypotheses over geological timescales: interactions between Mesozoic non-avian dinosaurs and cycads. *Biol. Rev.*, **84**: 73–89.

Campione, N.E. and Evans, D.C. 2011. Cranial growth and variation in edmontosaurs (Dinosauria: Hadrosauridae): implications for Latest Cretaceous megaherbivore diversity in North America. *PLoS One*, **6**: e25186.

Campione, N.E. and Holmes, R. 2006. The anatomy and homologies of the ceratopsid syncervical. *J. Vertebr. Paleontol.*, **26**: 1014–1017.

Chapman, R.E. 1990. Shape analysis in the study of dinosaur morphology. In *Dinosaur Systematics: Approaches and Perspectives* (K. Carpenter and P.J. Currie, eds.), pp. 21–42. Cambridge: Cambridge University Press.

Cheverud, J.M. 1996. Developmental integration and the evolution of pleiotropy. *Am. Zool.*, **36**: 44–50.

Cheverud, J.M. 2004. Modular pleiotropic effects of quantitative trait loci on morphological traits. In *Modularity in Development and Evolution* (G. Schlosser and G.P. Wagner, eds.), pp. 132–153. Chicago, IL: University of Chicago Press.

Cheverud, J.M., Hartman, S.E., Richtsmeier, J.T. and Atchley, W.R. 1991. A quantitative genetic analysis of localized morphology in mandibles of inbred mice using finite element scaling analysis. *J. Cran. Genet. Dev. Biol.*, **11**: 122–137.

Cheverud, J.M., Leamy, L.J. and Routman, E.J. 1997. Pleiotropic effects of individual gene loci on mandibular morphology. *Evolution*, **51**: 2004–2014.

Cheverud, J.M., Ehrich, T.H., Vaughn, T.T., Koreishi, S.F., Linsey, R.B. and Pletscher, L.S. 2004. Pleiotropic effects on mandibular morphology II: differential epistasis and genetic variation in morphological integration. *J. Exp. Zool.*, **302B**: 424–435.

Chinnery, B. 2004a. Morphometric analysis of evolutionary trends in the ceratopsian postcranial skeleton. *J. Vertebr. Paleontol.*, **24**: 591–609.

Chinnery, B.J. 2004b. Description of *Prenoceratops pieganensis* gen. et sp. nov. (Dinosauria: Neoceratopsia) from the Two Medicine Formation of Montana. *J. Vertebr. Paleontol.*, **24**: 572–590.

Chinnery, B.J. and Horner, J.R. 2007. A new neoceratopsian dinosaur linking North American and Asian taxa. *J. Vertebr. Paleontol.*, **27**: 625–641.

Claude, J. 2008. *Morphometrics with R*. New York: Springer.

Coria, R.A. and Salgado, L. 2005. Mid-Cretaceous turnover of saurischian dinosaur communities: evidence from the Neuquén Basin. *Geol. Soc. Lond. Spec. Publ.*, **252**: 317–327.

Dennis, K.J., Cochran, J.K., Landman, N.H. and Schrag, D.P. 2013. The climate of the Late Cretaceous: new insights from the application of the carbonate clumped isotope thermometer to Western Interior Seaway macrofossil. *Earth Planet. Sci. Lett.*, **362**: 51–65.

Dodson, P. 1976. Quantitative aspects of relative growth and sexual dimorphism in *Protoceratops*. *J. Paleontol.*, **50**: 929–940.

Dodson, P. 1993. Comparative craniology of the Ceratopsia. *Am. J. Sci.*, **293A**: 200–234.

Dodson, P. 1996. *The Horned Dinosaurs*. Princeton, NJ: Princeton University Press.

Dodson, P., Forster, C.A. and Sampson, S.D. 2004. Ceratopsidae. In *The Dinosauria*, 2nd edn. (D.B. Weishampel, P. Dodson and H. Osmólska, eds.), pp. 494–513. Berkeley, CA: University of California Press.

Ehrich, T.H., Vaughn, T.T., Koreishi, S.F., Linsey, R.B., Pletscher, L.S. and Cheverud, J.M. 2003. Pleiotropic effects on mandibular morphology II. Developmental morphological integration and differential dominance. *J. Exp. Zool.*, **296B**: 58–79.

Escoufier, Y. 1973. Le traitement des variables vectorielles. *Biometrics*, **29**: 751–760.

Evans, D.C. and Ryan, M.J. 2015. Cranial anatomy of *Wendiceratops pinhornensis* gen. et sp. nov., a centrosaurine ceratopsid (Dinosauria: Ornithischia) from the Oldman Formation (Campanian), Alberta, Canada, and the evolution of ceratopsid nasal ornamentation. *PLoS One*, **10**: e0130007.

Farke, A.A., Ryan, M.J., Barrett, P.M., Tanke, D.H., Braman, D.R., Loewen, M.A. *et al.* 2011. A new centrosaurine from the Late Cretaceous of Alberta and the evolution of parietal ornamentation in horned dinosaurs. *Acta Palaeontol. Pol.*, **56**: 691–702.

Farke, A.A., Maxwell, W.D., Cifelli, R.L. and Wedel, M.J. 2014. A ceratopsian dinosaur from the Lower Cretaceous of Western North America, and the biogeography of Neoceratopsia. *PLoS One*, **9**: e112055.

Farlow, J.O. and Dodson, P. 1975. The behavioral significance of frill and horn morphology in ceratopsian dinosaurs. *Evolution*, **29**: 353–361.

Felsenstein, J. 1985. Phylogenies and the comparative method. *Am. Nat.*, **125**: 1–15.

Fiorillo, A.R. and Tykoski, R.S. 2012. A new Maastrichtian species of the centrosaurine ceratopsid *Pachyrhinosaurus* from the North Slope of Alaska. *Acta Palaeontol. Pol.*, **57**: 561–573.

Foth, C. and Rauhut, O.W.M. 2013. Macroevolutionary and morphofunctional patterns in theropod skulls: a morphometric approach. *Acta Palaeontol. Pol.*, **58**: 1–16.

Fruciano, C., Franchini, P. and Meyer, A. 2013. Resampling-based approaches to study variation in morphological modularity. *PLoS One*, **8**: e69376.

Garland, T., Jr. 1992. Rate tests for phenotypic evolution using phylogenetically independent contrasts. *Am. Nat.*, **140**: 509–519.

Garland, T., Jr., Bennett, A. and Rezende, E.L. 2005. Phylogenetic approaches in comparative physiology. *J. Exp. Biol.*, **208**: 3015–3035.

Han, F., Forster, C.A., Clark, J.M. and Xu, X. 2015. A new taxon of basal ceratopsian from China and the early evolution of Ceratopsia. *PLoS One*, **10**: e0143369.

Hancock, J.M. and Kauffman, E.G. 1979. The great transgressions of the Late Cretaceous. *J. Geol. Soc. Lond.*, **136**: 175–186.

Handa, N., Watabe, M. and Tsogtbaatar, K. 2012. New specimens of *Protoceratops* (Dinosauria: Neoceratopsia) from the Upper Cretaceous in Udyn Sayr, southern Gobi area, Mongolia. *Paleontol. Res.*, **16**: 179–198.

Hay, W.W. 2008. Evolving ideas about the Cretaceous climate and ocean circulation. *Cretaceous Res.*, **29**: 725–753.

Hedrick, B.P. and Dodson, P. 2013. Lujiatun psittacosaurids: understanding individual and taphonomic variation using 3D geometric morphometrics. *PLoS One*, **8**: e69265.

Henderson, D.M. 2010. Skull shape as indicators of niche partitioning by sympatric chasmosaurine and centrosaurine dinosaurs. In *New Perspectives on Horned Dinosaurs* (M.J. Ryan, B.J. Chinnery-Algeier and D.A. Eberth, eds.), pp. 293–307. Bloomington, IN: Indiana University Press.

Hone, D.W.E. and Naish, D. 2013. The 'species recognition hypothesis' does not explain the presence and evolution of exaggerated structures in non-avian dinosaurs. *J. Zool.*, **290**: 172–180.

Hone, D.W.E., Naish, D. and Cuthill, I.C. 2012. Does mutual sexual selection explain the evolution of head crests in pterosaurs and dinosaurs? *Lethaia*, **45**: 139–156.

Kirkland, J.I. and DeBlieux, D.D. 2010. New basal centrosaurinae ceratopsian skull from the Wahweap Formation (Middle Campanian), Grand Staircase-Escalante Monument, Southern Utah. In *New Perspectives on Horned Dinosaurs* (M.J. Ryan, B.J. Chinnery-Algeier and D.A. Eberth, eds.), pp. 117–140. Bloomington, IN: Indiana University Press.

Klingenberg, C.P. 2009. Morphometric integration and modularity in configurations of landmarks: tools for evaluating a-priori hypotheses. *Evol. Dev.*, **11**: 405–421.

Klingenberg, C.P. and Gidaszewski, N.A. 2010. Testing and quantifying phylogenetic signals and homoplasy in morphometric data. *Syst. Biol.*, **59**: 245–261.

Klingenberg, C.P. and Leamy, L.J. 2001. Quantitative genetics of geometric shape in the mouse mandible. *Evolution*, **55**: 2342–2352.

Klingenberg, C.P. and Marugán-Lobón, J. 2013. Evolutionary covariation in geometric morphometric data: analyzing integration, modularity, and allometry in a phylogenetic Context. *Syst. Biol.*, **62**: 591–610.

Klingenberg, C.P., Leamy, L.J., Routman, E.J. and Cheverud, J.M. 2001. Genetic architecture of mandible shape in mice: effects of quantitative trait loci analyzed by geometric morphometrics. *Genetics*, **157**: 785–802.

Klingenberg, C.P., Barluenga, M. and Meye, A. 2003. Body shape variation in cichlid fishes of the *Amphilophus citrinellus* species complex. *Biol. J. Linn. Soc.*, **80**: 397–408.

Klingenberg, C.P., Leamy, L.J. and Cheverud, J.M. 2004. Integration and modularity of quantitative trait locus effects on geometric shape in the mouse mandible. *Genetics*, **166**: 1909–1921.

Knell, R.J. and Sampson, S. 2011. Bizarre structures in dinosaurs: species recognition or sexual selection? A response to Padian and Horner. *J. Zool.*, **283**: 18–22.

Lambert, O., Godefroit, P., Li, H., Shang, C. and Dong, Z.-M. 2001. A new species of *Protoceratops* (Dinosauria: Neoceratopsia) from the Late Cretaceous of Inner Mongolia (P.R. China). *Bull. Inst. R. Sc. N. B-S*, **71**: 5–28.

Leamy, L.J., Routman, E.J. and Cheverud, J.M. 2002. An epistatic genetic basis for fluctuating asymmetry of mandible size in mice. *Evolution*, **56**: 642–653.

Lee, Y.-N., Ryan, M.J. and Kobayashi, Y. 2011. The first ceratopsian from Korea. *Naturwissenschaften*, **98**: 39–49.

Lehman, T.M. 1990. The ceratopsian subfamily Chasmosaurinae: sexual dimorphism and

systematics. In *Dinosaur Systematics: Approaches and Perspectives* (K. Carpenter and P.J. Currie, eds.), pp. 211–229. Cambridge: Cambridge University Press.

Longrich, N.R. 2010. *Mojoceratops perifania*, a new chasmosaurine ceratopsid from the late Campanian of western Canada. *J. Paleontol.*, **84**: 681–694.

Longrich, N.R. 2013. *Judiceratops tigris*, a new horned dinosaur from the Middle Campanian Judith River Formation of Montana. *Bull. Peabody Mus. Nat. Hist.*, **54**: 51–65.

Lucas, S.G. 2006. The *Psittacosaurus* biochron, Early Cretaceous of Asia. *Cretaceous Res.*, **27**: 189–198.

Lupia, R., Crane, P.R. and Lidgard, S. 2000. Angiosperm diversification and Cretaceous environmental change. In *Biotic Responses to Global Change: The Last 145 Million Years* (S.J. Culver and P.F. Rawson, eds.), pp. 207–222. Cambridge: Cambridge University Press.

Maddison, W.P. and Maddison, D.R. 2011. Mesquite: A Modular System for Evolutionary Analysis, v. 2.75 [available at: http://mesquiteproject.org/mesquite/mesquite.html].

Maidment, S.C.R. and Barrett, P.M. 2011. A new specimen of *Chasmosaurus belli* (Ornithischia: Ceratopsidae), a revision of the genus, and the utility of postcrania in the taxonomy and systematics of ceratopsid dinosaurs. *Zootaxa*, **2963**: 1–47.

Maiorino, L., Farke, A.A., Piras, P., Ryan, M.J., Terris, K.M. and Kotsakis, T. 2013a. The evolution of squamosal shape in ceratopsid dinosaurs (Dinosauria, Ornithischia). *J. Vertebr. Paleontol.*, **33**: 1385–1393.

Maiorino, L., Farke, A.A., Piras, P. and Kotsakis, T. 2013b. Is *Torosaurus Triceratops*? Geometric morphometric evidence of Late Maastrichtian ceratopsid dinosaurs. *PLoS One*, **8**: e81608.

Maiorino, L., Farke, A.A., Kotsakis, T. and Piras, P. 2015a. Males resemble females: re-evaluating sexual dimorphism in *Protoceratops andrewsi* (Neoceratopsia, Protoceratopsidae). *PLoS One*, **10**: e0126464.

Maiorino, L., Farke, A.A., Kotsakis, T., Teresi, L. and Piras, P. 2015b. Variation in the shape and mechanical performance of the lower jaws in ceratopsid dinosaurs (Ornithischia, Ceratopsia). *J. Anat.*, **227**: 631–646.

Makovicky, P.J. 2002. Taxonomic revision and phylogenetic relationships of basal *Neoceratopsia* (Dinosauria: Ornithischia). PhD thesis, Columbia University, New York.

Makovicky, P.J. 2012. Marginocephalia. In *The Complete Dinosaur* (M.K. Brett-Surman, T.R. Holtz, Jr. and J.O. Farlow, eds.), pp. 527–549. Bloomington, IN: Indiana University Press.

Makovicky, P.J. and Norell, M.A. 2006. *Yamaceratops dorngobiensis*, a new primitive ceratopsian (Dinosauria: Ornithischia) from the Cretaceous of Mongolia. *Am. Mus. Nov.*, **3530**: 1–42.

Mallon, J.C. and Anderson, J.S. 2013. Skull ecomorphology of megaherbivorous dinosaurs from the Dinosaur Park Formation (Upper Campanian) of Alberta, Canada. *PLoS One*, **8**: e67182.

Mallon, J.C. and Anderson, J.S. 2014. Implications of beak morphology for the evolutionary paleoecology of the megaherbivorous dinosaurs from the Dinosaur Park Formation (Upper Campanian) of Alberta, Canada. *Palaeogeogr. Palaeoclimatol. Palaeoecol.*, **394**: 29–41.

Mallon, J.C. and Anderson, J.S. 2015. Jaw mechanics and evolutionary paleoecology of megaherbivorous dinosaurs from the Dinosaur Park Formation (Upper Campanian) of Alberta, Canada. *J. Vertebr. Paleontol.*, **35**: e904323.

Mallon, J.C., Holmes, R., Anderson, J.S., Farke, A.A. and Evans, D.C. 2014. New information on the rare horned dinosaur *Arrhinoceratops brachyops* (Ornithischia: Ceratopsidae) from the Upper Cretaceous of Alberta, Canada. *Can. J. Earth Sci.*, **51**: 1–18.

Marcolini, F., Piras, P. and Martin, R.A. 2009. Testing evolutionary dynamics on first lower molars of Pliocene *Ogmodontomys* (Arvicolidae, Rodentia) from the Meade Basin of southwestern Kansas (USA): a landmark-based approach. *Palaios*, **24**: 535–543.

Marcus, L.F., Hingst-Zaher, E. and Zaher, H. 2000. Application of landmarks morphometrics to skull representing the orders of living mammals. *Hystrix*, **11**: 27–47.

Márquez, E.J. 2008. A statistical framework for testing modularity in multidimensional data. *Evolution*, **62**: 2688–2708.

Maryańska, T. and Osmólska, H. 1975. Protoceratopsidae (Dinosauria) of Asia. *Palaeontol. Pol.*, **33**: 133–181.

Mayr, E. 1970. *Populations, Species, and Evolution: An Abridgment of Animal Species and Evolution*. Cambridge, MA: Belknap Press.

Meloro, C. and Slater, G.J. 2012. Covariation in the skull modules of cats: the challenge of growing saber-like canines. *J. Vertebr. Paleontol.*, **32**: 677–685.

Meloro, C., Raia, P., Piras, P., Barbera, C. and O'Higgins, P. 2008. The shape of the mandibular corpus in large fissiped carnivores: allometry, function and phylogeny. *Zool. J. Linn. Soc.*, **154**: 832–845.

Meloro, C., Raia, P., Carotenuto, F. and Cobb, S.N. 2011. Phylogenetic signal, function and integration in the subunits of the carnivoran mandible. *Evol. Biol.*, **38**: 465–475.

Mitteroecker, P. and Bookstein, F. 2008. The evolutionary role of modularity and integration in the hominoid cranium. *Evolution*, **62**: 943–958.

Mitteroecker, M., Gunz, P. and Bookstein, F.L. 2005. Heterochrony and geometric morphometrics: a comparison of cranial growth in *Pan paniscus* versus *Pan troglodytes*. *Evol. Dev.*, **7**: 244–258.

Monteiro, L.R. 2000. Geometric morphometrics and the development of complex structures: ontogenetic changes in scapular shape of dasypodid armadillos. *Hystrix*, **11**: 91–98.

Mullin, S.K. and Taylor, P.J. 2002. The effects of parallax on geometric morphometric data. *Comput. Biol. Med.*, **32**: 455–464.

Neenan, J.M., Ruta, M., Clack, J.A. and Rayfield, E.J. 2014. Feeding biomechanics in *Acanthostega* and across the fish–tetrapod transition. *Proc. R. Soc. Lond. B: Biol. Sci.*, **281**: 20132689.

Nessov, L.A. 1995. *Dinosaurs of Northern Eurasia: New Data about Assemblages, Ecology and Paleobiogeography*. St. Petersburg: Izdatelstvo Sankt-Peterburgskogo Universiteta (in Russian), 156 pp.

Nessov, L.A., Kaznyshkina, L.F. and Cherepanov, G.O. 1989. Ceratopsian dinosaurs and crocodiles of the middle Mesozoic of Asia. In *Theoretical and Applied Aspects of Modern Paleontology* (T.N. Bogdanova and L.I. Kozhatsky, eds.), pp. 142–149. Leningrad: Nauka.

Oksanen, J., Blanchet, F.G., Kindt, R., Legendre, P., Minchin, P.R., O'Hara, R.B. *et al.* 2011. Vegan: Community Ecology Package. R package, v. 2.0-2 [available at: http://CRAN.R-project.org/package = vegan].

O'Meara, B.C., Ané, C., Sanderson, M.J. and Wainwright, P.C. 2006. Testing for different rates of continuous trait evolution using likelihood. *Evolution*, **60**: 922–933.

Ösi, A., Butler, R.J. and Weishampel, D.B. 2010. A Late Cretaceous ceratopsian dinosaur from Europe with Asian affinities. *Nature*, **465**: 466–468.

Ostrom, J.H. 1966. Functional morphology and evolution of the ceratopsian dinosaurs. *Evolution*, **20**: 290–308.

Ostrom, J.H. and Wellnhofer, P. 1986. The Munich specimen of *Triceratops* with a revision of the genus. *Zitteliana*, **14**: 111–158.

Padian, K. and Horner, J.R. 2011. The evolution of 'bizarre structures' in dinosaurs: biomechanics, sexual selection, social selection or species recognition? *J. Zool.*, **283**: 3–17.

Padian, K. and Horner, J.R. 2014. The species recognition hypothesis explains exaggerated structures in non-avialan dinosaurs better than sexual selection does. *C. R. Palevol.*, **13**: 97–107.

Perez, S.I., Bernal, V. and Gonzalez, P.N. 2006. Differences between sliding semi-landmark methods in geometric morphometrics, with an application to human craniofacial and dental variation. *J. Anat.*, **208**: 769–784.

Piras, P., Maiorino, L., Raia, P., Marcolini, F., Salvi, D., Vignoli, L. *et al.* 2010. Functional and phylogenetic constraints in Rhinocerotinae craniodental morphology. *Evol. Ecol. Res.*, **12**: 897–928.

Piras, P., Salvi, D., Ferrara, G., Maiorino, L., Delfino, M., Pedde, L. *et al.* 2011. The role of post-natal ontogeny in the evolution of phenotypic diversity in *Podarcis* lizards. *J. Evol. Biol.*, **24**: 2705–2720.

Piras, P., Maiorino, L., Teresi, L., Meloro, C., Lucci, F., Kotsakis, T. *et al.* 2013. Bite of the cats: relationships between functional integration and mechanical performance as revealed by mandible geometry. *Syst. Biol.*, **62**: 878–900.

Polly, P.D. 2005. Development and phenotypic correlations: the evolution of tooth shape in *Sorex araneus*. *Evol. Dev.*, **7**: 29–41.

Raia, P., Passaro, P., Carotenuto, F., Maiorino, L., Piras, P., Teresi, L. *et al.* 2015. Cope's rule and the universal scaling law of ornament complexity. *Am. Nat.*, **186**: 165–-175.

Revell, L.J. 2012. phytools: an R package for phylogenetic comparative biology (and other things). *Meth. Ecol. Evol.*, **3**: 217–223.

Rohlf, F.J. 2001. Comparative methods for the analysis of continuous variables: geometric interpretations. *Evolution,* **55**: 2143–2160.

Rohlf, F.J. 2006. A comment on phylogenetic corrections. *Evolution*, **60**: 1509–1515.

Rohlf, F.J. 2013. tpsDig2, v. 2.17 [freeware available at: http://life.bio.sunysb.edu/morph/].

Rohlf, F.J. and Corti, M. 2000. Use of two-block partial least squares to study covariation in shape. *Syst. Biol.*, **49**: 740–753.

Rohlf, F.J., Loy, A. and Corti, M. 1996. Morphometrics analysis of Old World Talpidae (Mammalia, Insectivora) using partial-warp scores. *Syst. Biol.*, **45**: 344–362.

Royer, D.L., Berner, R.A. and Beerling, D.J. 2001. Phanerozoic atmospheric CO_2 change: evaluating geochemical and Paleobiological approaches. *Earth-Sci. Rev.*, **54**: 349–392.

Ryan, M.J. 2007. A new basal centrosaurine ceratopsid from the Oldman Formation, Southeastern Alberta. *J. Paleontol.*, **81**: 376–396.

Ryan, M.J., Evans, D.C., Currie, P.J., Brown, C.M. and Brinkman, D. 2012a. New leptoceratopsids from the Upper Cretaceous of Alberta, Canada. *Cretaceous Res.*, **35**: 69–80.

Ryan, M.J., Evans, D.C. and Shepherd, K.M. 2012b. A new ceratopsid from the Foremost Formation (middle Campanian) of Alberta. *Can. J. Earth Sci.*, **49**: 1251–1262.

Sampson, S.D. 1995. Two new horned dinosaurs from the upper Cretaceous Two Medicine Formation of Montana, with a phylogenetic analysis of the Centrosaurinae (Ornithischia: Ceratopsidae). *J. Vertebr. Paleontol.*, **15**: 743–760.

Sampson, S.D. and Loewen, M.A. 2010. Unraveling a radiation: a review of the diversity, stratigraphy, distribution, biogeography, and evolution of horned dinosaurs (Ornithischia: Ceratopsidae). In *New Perspectives on Horned Dinosaurs* (M.J. Ryan, B.J. Chinnery-Allgeier and D.A. Eberth, eds.), pp. 405–427. Bloomington, IN: Indiana University Press.

Sampson, S.D., Loewen, M.A., Farke, A.A., Roberts, E.M., Forster, C.A., Smith, J.A. *et al.* 2010. New horned dinosaurs from Utah provide evidence for intracontinental dinosaur endemism. *PLoS One*, **5**: e12292.

Sampson, S.D., Lund, E.K., Loewen, M.A., Farke, A.A. and Clayton, K.E. 2013. A remarkable short-snouted horned dinosaur from the Late Cretaceous (Late Campanian) of southern Laramidia. *Proc. R. Soc. Lond. B: Biol. Sci.*, **280**: 20131186.

Schlager, S. 2013. Morpho: calculations and visualizations related to geometric morphometrics. R package v. 0.23.3 [available at: http://CRAN.R-project.org/package = Morpho].

Sereno, P.C. 1990. New data on parrot-beaked dinosaurs (*Psittacosaurus*). In *Dinosaur Systematics: Approaches and Perspectives* (K. Carpenter and P.J. Currie, eds.), pp. 203–210. Cambridge: Cambridge University Press.

Sereno, P.C. 2010. Taxonomy, cranial morphology, and relationships of parrot-beaked dinosaurs (Ceratopsia: *Psittacosaurus*). In *New Perspectives on Horned Dinosaurs* (M.J. Ryan, B.J. Chinnery-Allgeier and D.A. Eberth, eds.), pp. 21–58. Bloomington, IN: Indiana University Press.

Sereno, P.C., Zhao, X.-J., Brown, L. and Tan, L. 2007. New psittacosaurid highlights skull enlargement in horned dinosaurs. *Acta Palaeontol. Pol.*, **52**: 275–284.

Sereno, P.C., Zhao, X. and Tan, L. 2010. A new psittacosaur from Inner Mongolia and the parrot-like structure and function of the psittacosaur skull. *Proc. R. Soc. Lond. B: Biol. Sci.*, **277**: 199–209.

Sloan, L.C. and Barron, E.J. 1990. 'Equable' climates during Earth history? *Geology*, **18**: 489–492.
Soltis, D.E., Soltis, P.S., Endress, P.K. and Chase, M.W. 2005. *Phylogeny and Evolution of the Angiosperms*. Sunderland, MA: Sinauer Associates.
Stanley, S.M. 2009. *Earth System History*, 3rd edn. New York: W.H. Freeman.
Sun, G., Dilcher, D.L., Wang, H. and Chen, Z. 2011. A eudicot from the Early Cretaceous of China. *Nature*, **471**: 625–628.
Swisher, C.C., Wang, Y.Q., Wang, X., Xu, X. and Wang, Y. 1999. Cretaceous age for the feathered dinosaurs of Liaoning, China. *Nature*, **400**: 58–61.
Swisher, C.C., Wang, X., Zhou, Z., Wang, Y.Q., Jin, F., Zhang, J.Y. *et al.* 2002. Further support for a Cretaceous age for the feathered-dinosaur beds of Liaoning, China: New $^{40}Ar/^{39}Ar$ dating of the Yixian and Tuchengzi formations. *Chinese Sci. Bull.*, **47**: 135–138.
Tanoue, K., Grandstaff, B.S., You, H.-L. and Dodson, P. 2009. Jaw mechanics in basal Ceratopsia (Ornithischia, Dinosauria). *Anat. Rec.*, **292**: 1352–1369.
Tanoue, K., You, H.-L. and Dodson, P. 2010. Mandibular anatomy in basal Ceratopsia. In *New Perspectives on Horned Dinosaurs* (M.J. Ryan, B.J. Chinnery-Allgeier and D.A. Eberth, eds.), pp. 234–250. Bloomington, IN: Indiana University Press.
Thomas, G.H. and Freckleton, R.P. 2012. MOTMOT: models of trait macroevolution on trees. *Meth. Ecol. Evol.*, **3**: 145–151.
Thomas, G.H., Meiri, S. and Phillimore, A.B. 2009. Body size diversification in *Anolis*: novel environment and island effects. *Evolution*, **63**: 2017–2030.
Tiffney, B.H. 2004. Vertebrate dispersal of seed plants through time. *Annu. Rev. Ecol. Evol. Syst.*, **35**: 1–29.
VanBuren, C.S., Campione, N.E. and Evans, D.C. 2015. Head size, weaponry, and cervical adaptation: testing craniocervical evolutionary hypotheses in Ceratopsia. *Evolution*, **69**: 1729–1744.
Weishampel, D.B. and Jianu, C.-M. 2000. Plant-eaters and ghost lineages: dinosaurian herbivory revisited. In *Evolution of Herbivory in Terrestrial Vertebrates: Perspectives from the Fossil Record* (H.-D. Sues, ed.), pp. 123–143. Cambridge: Cambridge University Press.
Wick, S.L. and Lehman, T.M. 2013. A new ceratopsian dinosaur from the Javelina Formation (Maastrichtian) of West Texas and implications for chasmosaurine phylogeny. *Naturwissenschaften*, **100**: 667–682.
Wolfe, D.G. and Kirkland, J.I. 1998 *Zuniceratops christopheri* n. gen. et n. sp., a ceratopsian dinosaur from the Moreno Hill Formation (Cretaceous, Turonian) of West-Central New Mexico. *NM Mus. Nat. Hist. Sci. Bull.*, **14**: 303–317.
Wu, X.-C., Brinkman, D.B., Eberth, D.A. and Braman, D.R. 2007. A new ceratopsid dinosaur (Ornithischia) from the uppermost Horseshoe Canyon Formation (Upper Maastrichtian), Alberta, Canada. *Can. J. Earth Sci.*, **44**: 1243–1265.
Xu, X., Makovicky, P.J., Wang, X.-L., Norell, M.A. and You, H.-L. 2002. A ceratopsian dinosaur from China and the early evolution of Ceratopsia. *Nature*, **416**: 314–317.
Xu, X., Forster, C.A., Clark, J.M. and Mo, J. 2006. A basal ceratopsian with transitional features from the Late Jurassic of northwestern China. *Proc. R. Soc. Lond. B: Biol. Sci.*, **273**: 2135–2140.
Xu, X., Wang, K., Zhao, X., Sullivan, C. and Chen, S. 2010a. A new leptoceratopsid (Ornithischia: Ceratopsia) from the Upper Cretaceous of Shandong, China and its implications for neoceratopsian evolution. *PLoS One*, **5**: e13835.
Xu, X., Wang, K., Zhao, X. and Li, D. 2010b. First ceratopsid dinosaur from China and its biogeographical implications. *Chinese Sci. Bull.*, **55**: 1631–1635.
You, H.-L. and Dodson, P. 2004. Basal Ceratopsia. In *The Dinosauria*, 2nd edn. (D.B. Weishampel, P. Dodson and H. Osmólska, eds.), pp. 478–593. Berkeley, CA: University of California Press.
You, H.-L. and Xu, X. 2005. An adult specimen of *Hongshanosaurus houi* (Dinosauria: Psittacosauridae) from the Lower Cretaceous of Western Liaoning Province, China. *Acta Geol. Sin-Engl.*, **79**: 168–173.

You, H.-L., Li, D., Ji, Q., Lamanna, M.C. and Dodson, P. 2005. On a new genus of basal neoceratopsian Dinosaur from the Early Cretaceous of Gansu Province, China. *Acta Geol. Sin-Engl*. **79**: 593-597.

You, H.-L., Xu, X. and Wang, X. 2003. A new genus of Psittacosauridae (Dinosauria: Ornithopoda) and the origin and early evolution of Marginocephalian dinosaurs. *Acta Geol. Sin-Engl.*, **77**: 15–20.

Young, M.T., Brusatte, S.L., Ruta, M. and De Andrade, M.B. 2010. The evolution of Metriorhynchoidea (Mesoeucrocodylia, Thalattosuchia): an integrated approach using geometric morphometrics, analysis of disparity, and biomechanics. *Zool. J. Linn. Soc.*, **158**: 801–859.

Zelditch, M.L., Wood, A.R. and Swiderski, D.L. 2009. Building developmental integration into functional systems: function-induced integration of mandibular shape. *Evol. Biol.*, **36**: 71–87.

Zelditch, M.L., Swiderski, D.L. and Sheets, H.D. 2012. *Geometric Morphometrics for Biologists: A Primer*. Amsterdam: Elsevier Academic Press.

Zhao, X. 1983. Phylogeny and evolutionary stages of Dinosauria. *Acta Palaeontol. Pol.*, **28**: 295–306.

Zhao, X., Cheng, Z. and Xu, X. 1999. The earliest ceratopsian from the Tuchengzi Formation of Liaoning. China. *J. Vertebr. Paleontol.*, **19**: 681–691.

Zhao, X., Cheng, Z., Xu, X. and Makovicky, P.J. 2006. A new ceratopsian from the Upper Jurassic Houcheng Formation of Hebei, China. *Acta Geol. Sin-Engl.*, **80**: 467–473.

Zheng, W., Jin, X. and Xu, X. 2015. A psittacosaurid-like basal neoceratopsian from the Upper Cretaceous of central China and its implications for basal ceratopsian evolution. *Sci. Rep.*, **5**: 14190.